TeV Halos: Past, Present and Future

(Observations, Models, and Implications)

TIM LINDEN

Stockholm University

- Geminga
  - 4.9×10^{-14} TeV^{-1} cm^{-2} s^{-1} (7 TeV)
  - 1.4×10^{31} TeV s^{-1} (7 TeV)
  - 25 pc extension
  - 300 kyr

- Monogem
  - 2.3×10^{-14} TeV^{-1} cm^{-2} s^{-1} (7 TeV)
  - 1.1×10^{31} TeV s^{-1} (7 TeV)
  - 25 pc extension
  - 110 kyr

EARLY LESSONS

- 1.) Pulsars are highly efficient e^+e^- accelerators.
- 2.) Pulsar e^+e^- are not confined in the source.
- 3.) Regions near sources have unusually low diffusion coefficients.

A NEW SOURCE CLASS

TeV Halos are much larger than PWN, especially at low spin down energies and large ages.

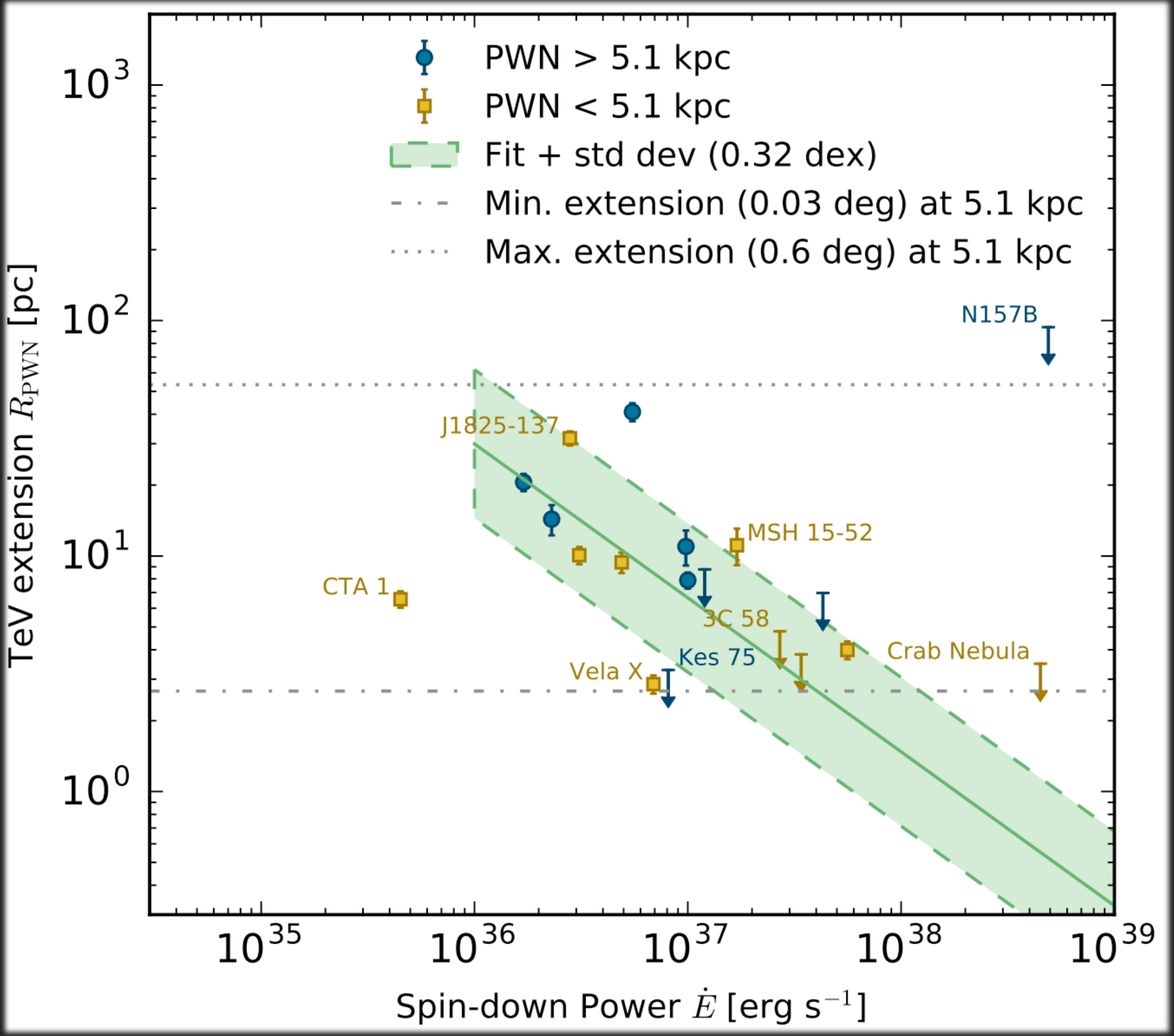

NOTE: The size of halos has the opposite time-dependence as the X-Ray PWN.

$$R_{\mathrm{PWN}} \simeq 1.5 \left(\frac{\dot{E}}{10^{35}\,\mathrm{erg/s}}\right)^{1/2} \times \left(\frac{n_{\mathrm{gas}}}{1\,\mathrm{cm}^{-3}}\right)^{-1/2} \left(\frac{v}{100\,\mathrm{km/s}}\right)^{-3/2} \mathrm{pc}$$

EARLY LESSONS - THE GEMINGA-CENTRIC MODEL

ATNF Name	Dec. (°)	Distance (kpc)	Age (kyr)	Spindown Lum. (erg s^{-1})	Spindown Flux (erg s^{-1} kpc^{-2})	2HWC
J0633+1746	17.77	0.25	342	3.2e34	4.1e34	2HWC J0631+169
B0656+14	14.23	0.29	111	3.8e34	3.6e34	2HWC J0700+143
B1951+32	32.87	3.00	107	3.7e36	3.3e34	—
J1740+1000	10.00	1.23	114	2.3e35	1.2e34	—
J1913+1011	10.18	4.61	169	2.9e36	1.1e34	2HWC J1912+099
J1831-0952	-9.86	3.68	128	1.1e36	6.4e33	2HWC J1831-098
J2032+4127	41.45	1.70	181	1.7e35	4.7e33	2HWC J2031+415
B1822-09	-9.58	0.30	232	4.6e33	4.1e33	—
B1830-08	-8.45	4.50	147	5.8e35	2.3e33	—
J1913+0904	9.07	3.00	147	1.6e35	1.4e33	—
B0540+23	23.48	1.56	253	4.1e34	1.4e33	—

- **Make One Key Assumption:**

- **The following correlation is consistent with the data.**

$$\phi_{\mathrm{TeV\ halo}} = \left(\frac{\dot{E}_{\mathrm{psr}}}{\dot{E}_{\mathrm{Geminga}}}\right)\left(\frac{d^2_{\mathrm{Geminga}}}{d^2_{\mathrm{psr}}}\right)\phi_{\mathrm{Geminga}}$$

- **Note: Using Monogem would increases fluxes by nearly a factor of 2. The power law of this correlation doesn’t greatly affect the results.**

THE KEY RESULTS - POSITRON EXCESS

- **What were the uncertainties in pulsar models?**
  - **I: The e^+e^- production efficiency?**

Profumo (0812.4457); Malyshev et al. (0903.1310)

%. A quantitative discussion of plausible values for $f_{e^\pm}$ was recently given in Ref. [38]. We shall not review their discussion here, but Ref. [38] argues (see in particular their very informative App. B and C) that in the context of a standard model for the pulsar wind nebulae, a reasonable range for $f_{e^\pm}$ falls between 1% and 30%.

  - **II: The e^+e^- spectrum.**

Hooper et al. (0810.1527)

part of their energy adiabatically because of the expansion of the wind. The energy spectrum injected by a single pulsar depends on the environmental parameters of the pulsar, but some attempts to calculate the average spectrum injected by a population of mature pulsars suggest that the spectrum may be relatively hard, having a slope of ~1.5-1.6 [18]. This spectrum, however, results from a complex interplay of individual pulsar spectra, of the spatial and age distributions of pulsars in the Galaxy, and on the assumption that the chief channel for pulsar spin down is magnetic dipole radiation. Due to the related uncertainties, variations from this injection spectra cannot be ruled out. Typically, one concentrates the attention on pulsars of age $\sim 10^5$ years because younger pulsars are likely to still

  - **III: The propagation of e^+e^- to Earth.**

Malyshev et al. (0903.1310)

The observed spectrum on Earth of electrons and positrons injected by pulsars is also strongly dependent on propagation effects. In particular, the observed cutoff in the flux of electrons from a pulsar can be much smaller than the injection cutoff due to energy losses ("cooling") during propagation. We define the cooling break, $E_{\rm br}(t)$, as the maximal energy electrons can have after propagating for time t. Since – as stated above – the typical

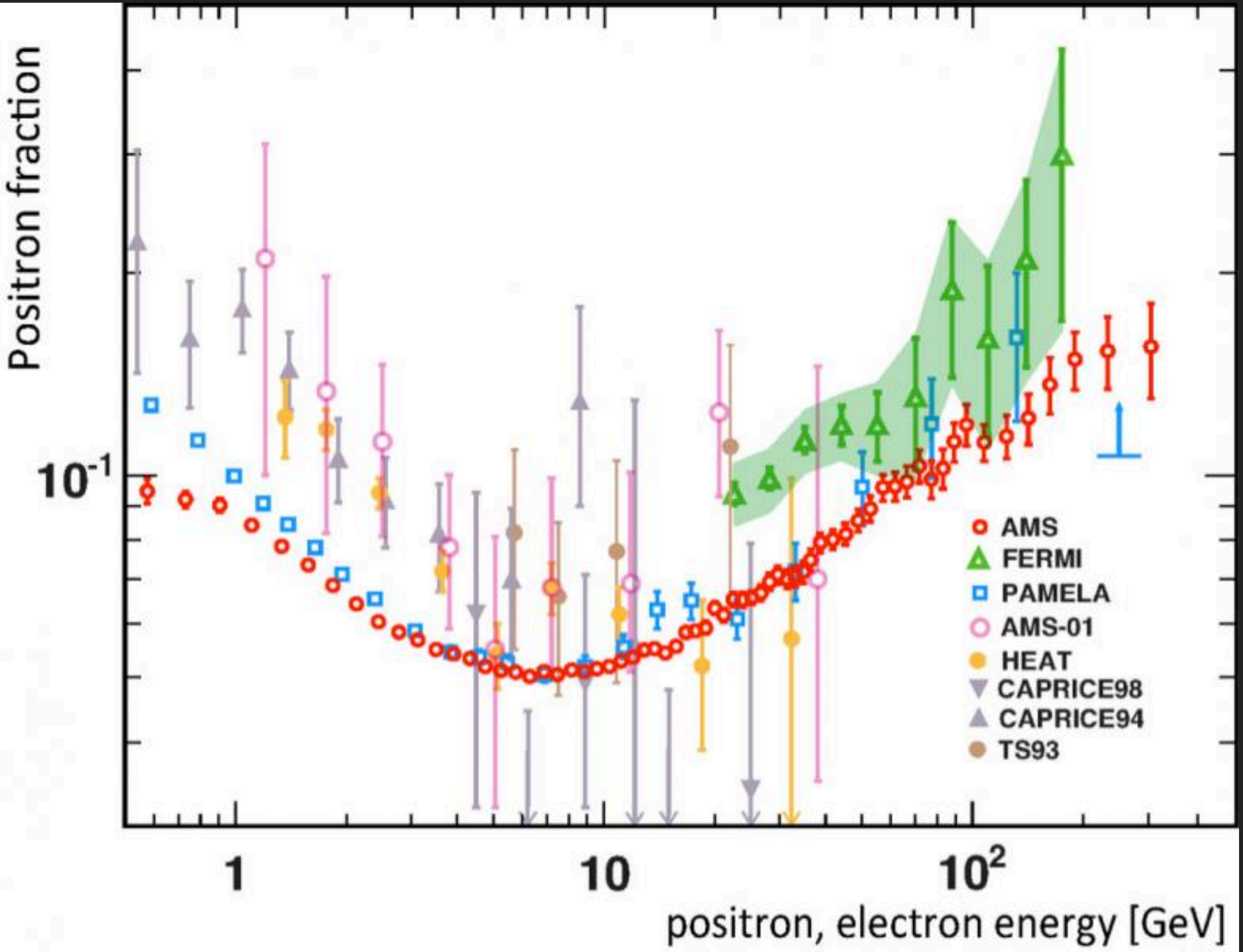

THE KEY RESULTS - MISSING TEV HALOS

- Radio pulsars are beamed!

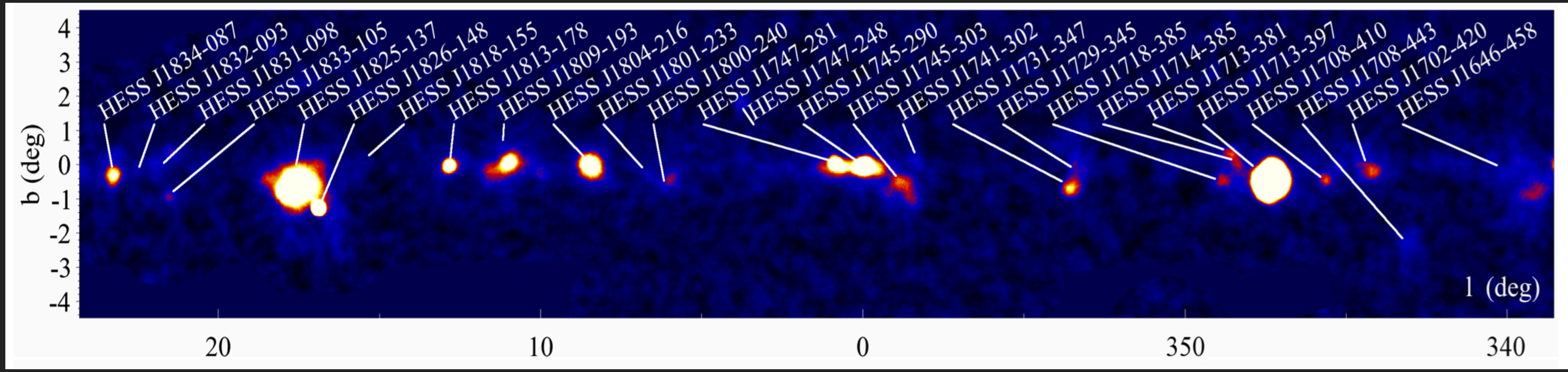

- Beaming fraction is small

Tauris & Manchester (1998)

$$f = \left[1.1 \left(\log_{10} \left(\frac{\tau}{100\ \mathrm{Myr}} \right) \right)^2 + 15 \right] \%$$

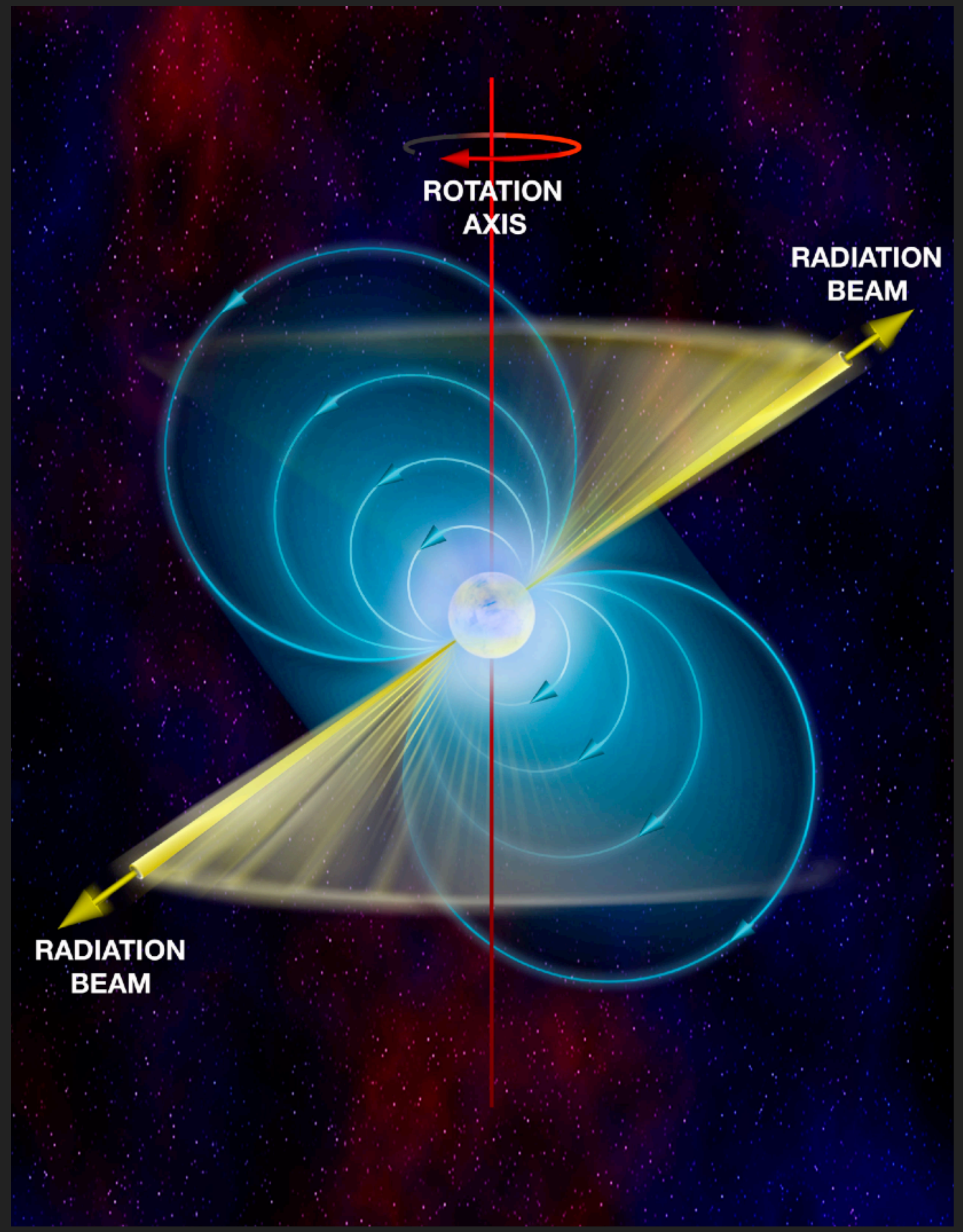

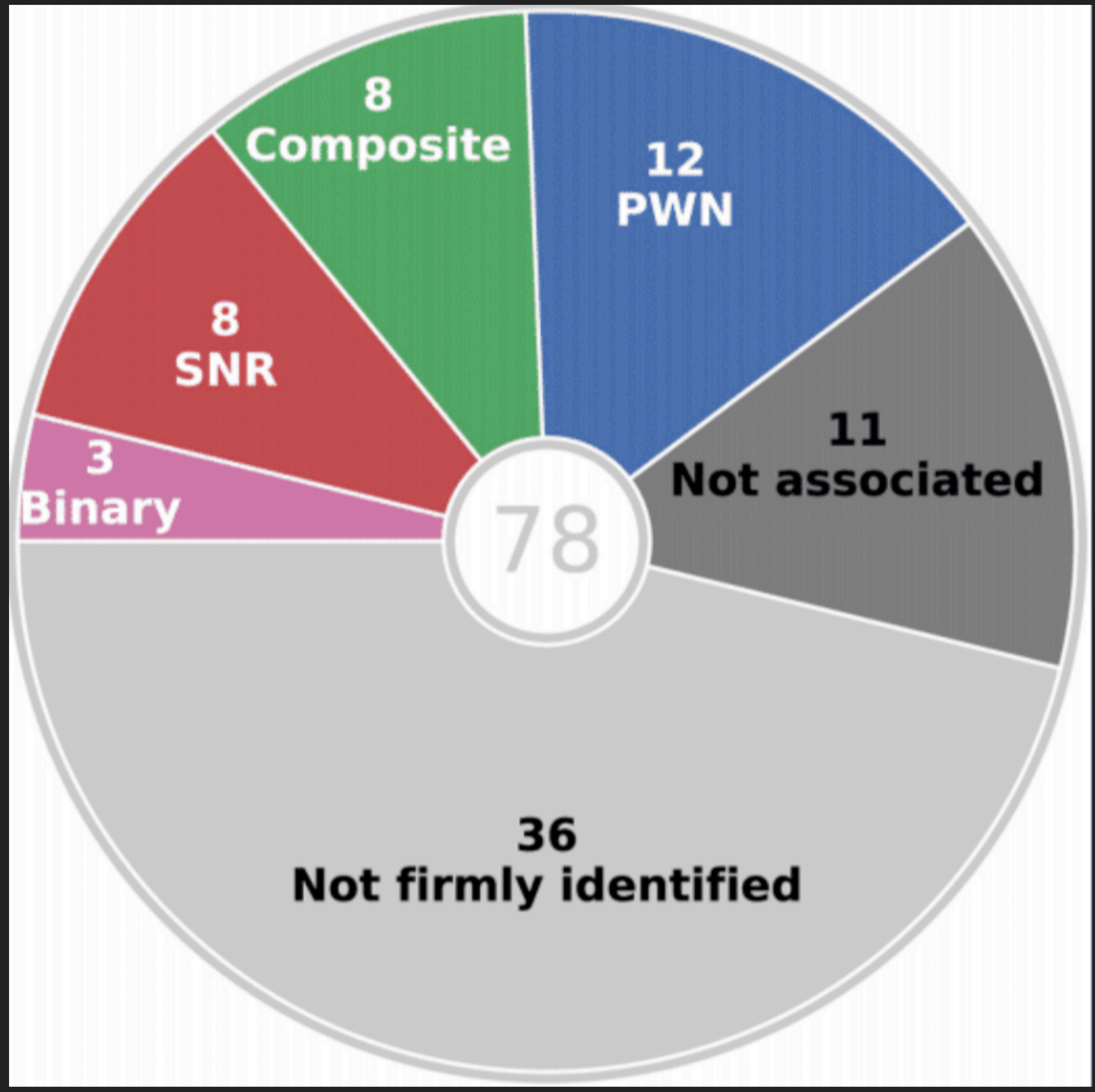

- This varies between 15-30%.

- Most pulsars are unseen in radio!

THE KEY RESULTS - DIFFUSE TEV EMISSION

- If all convert a similar fraction of their spin down power to e+e- pairs as Geminga, then TeV halos naturally explain this observation.

- Note - “Halo” is not needed
  - Pulsar efficiency ~10%
  - Power must escape PWN

Linden & Buckman (2017; 1707.01905)

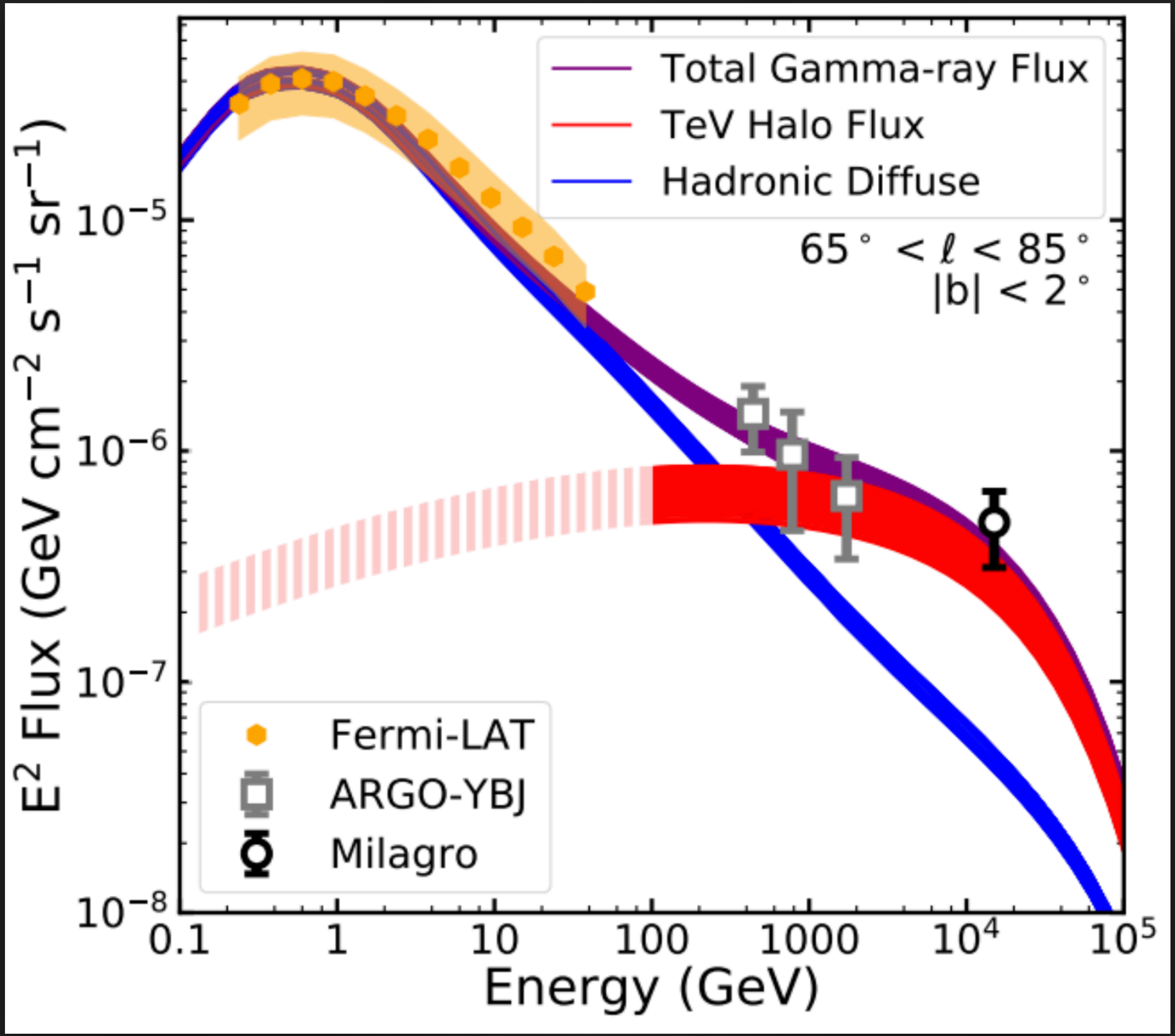

IMPLICATION: DIFFUSE TEV GAMMA-RAYS

- TeV halos naturally explain the spectrum and intensity of this emission.
- Multiple halos observed with $E^{-2.0}$ spectra.
- Note - “Halo” is not needed
  - Pulsar efficiency ~10%
  - Power must escape PWN

Fang & Murase (2021; 2104.09491)

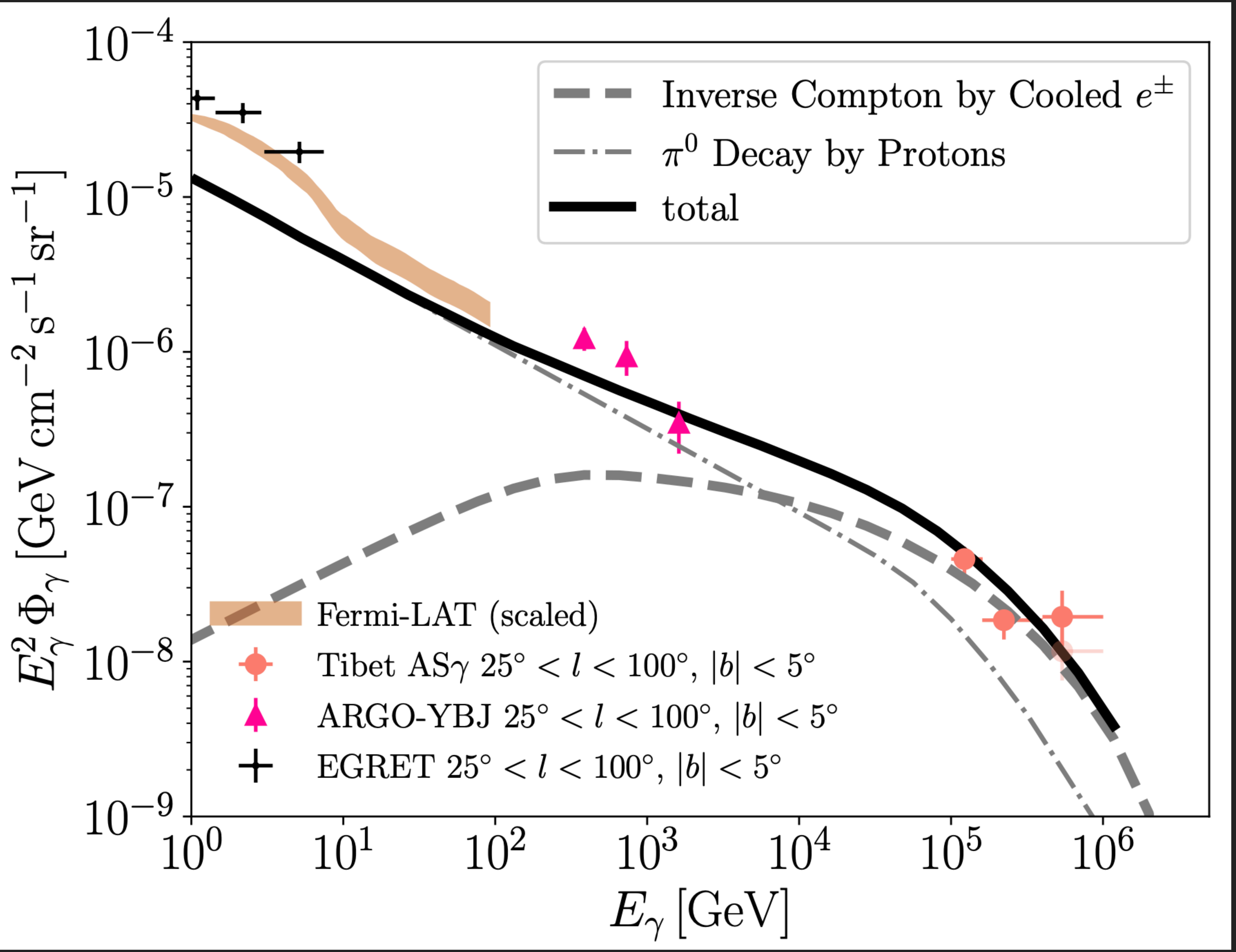

Tibet ASγ data

INVISIBLE ELEPHANT IN THE ROOM

IceCube Collaboration (2023)

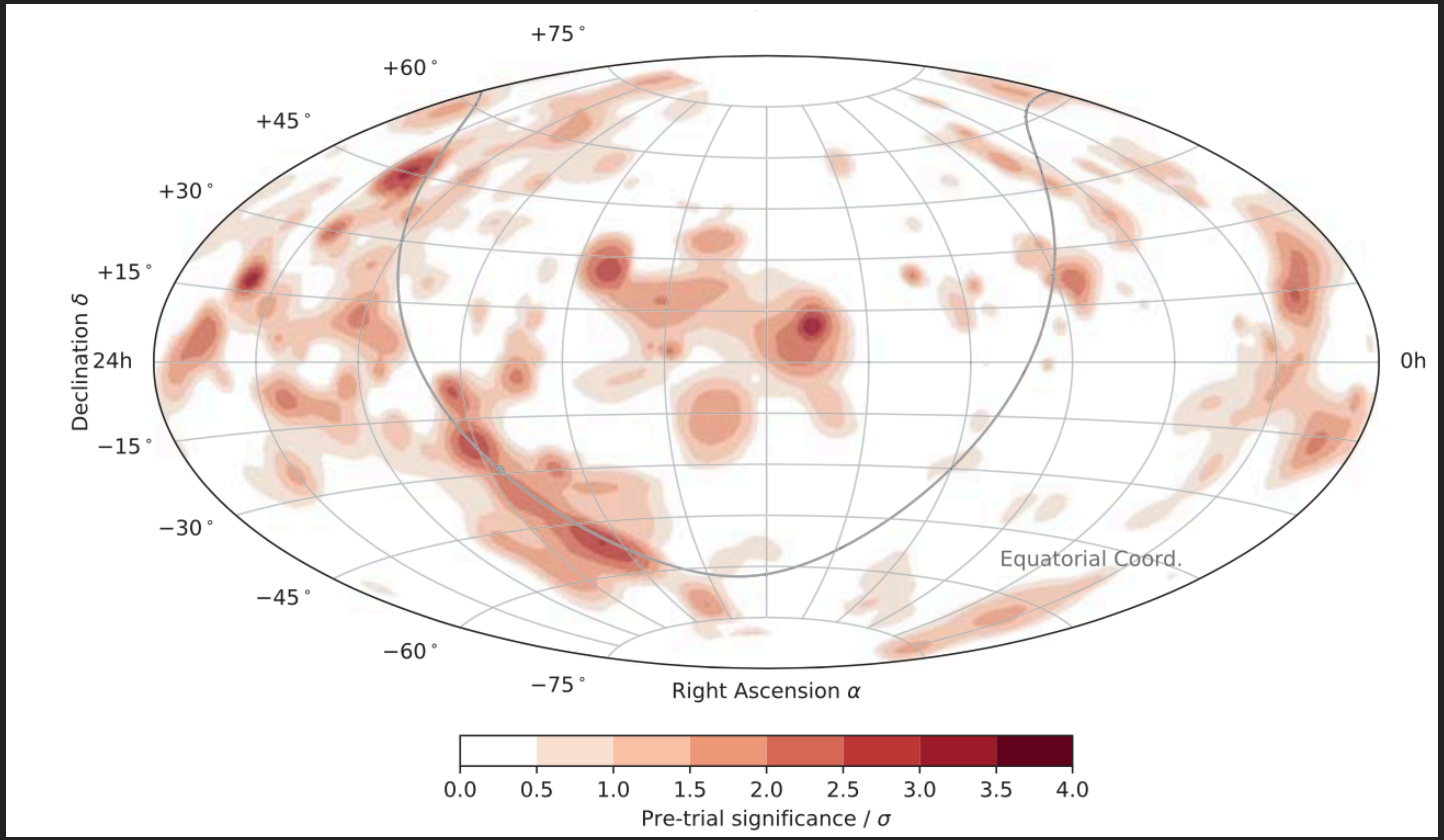

- IceCube detection of a galactic neutrino flux – with a normalization that is ~4x brighter than expectations from the Fermi-LAT extrapolation.

INVISIBLE ELEPHANT IN THE ROOM

Fang et al. (2023; 2306.17275)

- If the IceCube neutrino flux from the galaxy is higher, then the gamma-ray flux from hadronic processes (i.e., not halos) could also be higher.
- In Fang et al. this is capable of producing the diffuse galactic gamma-ray emission

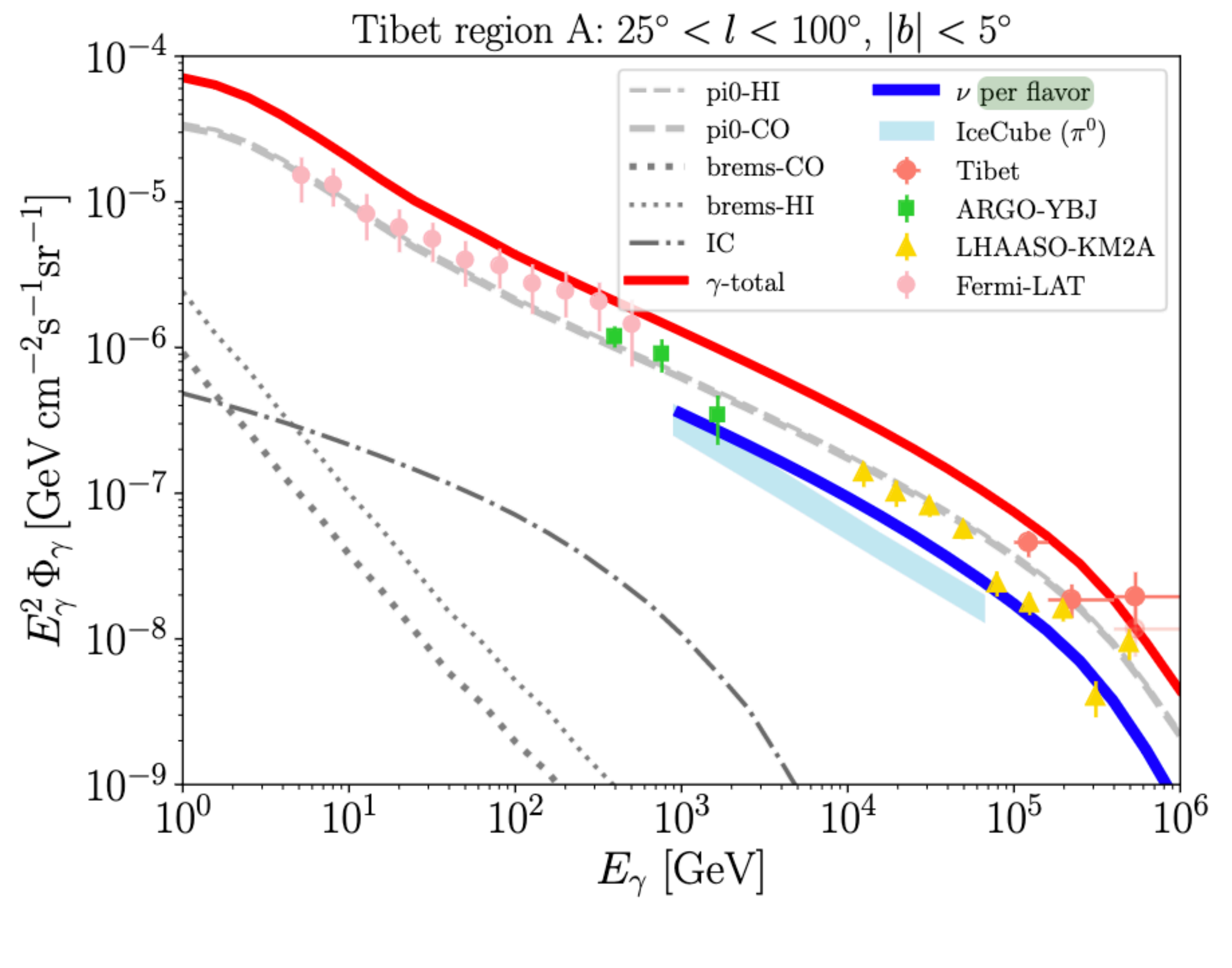

INVISIBLE ELEPHANT IN THE ROOM

Shao et al. (2023; 2307.01038)

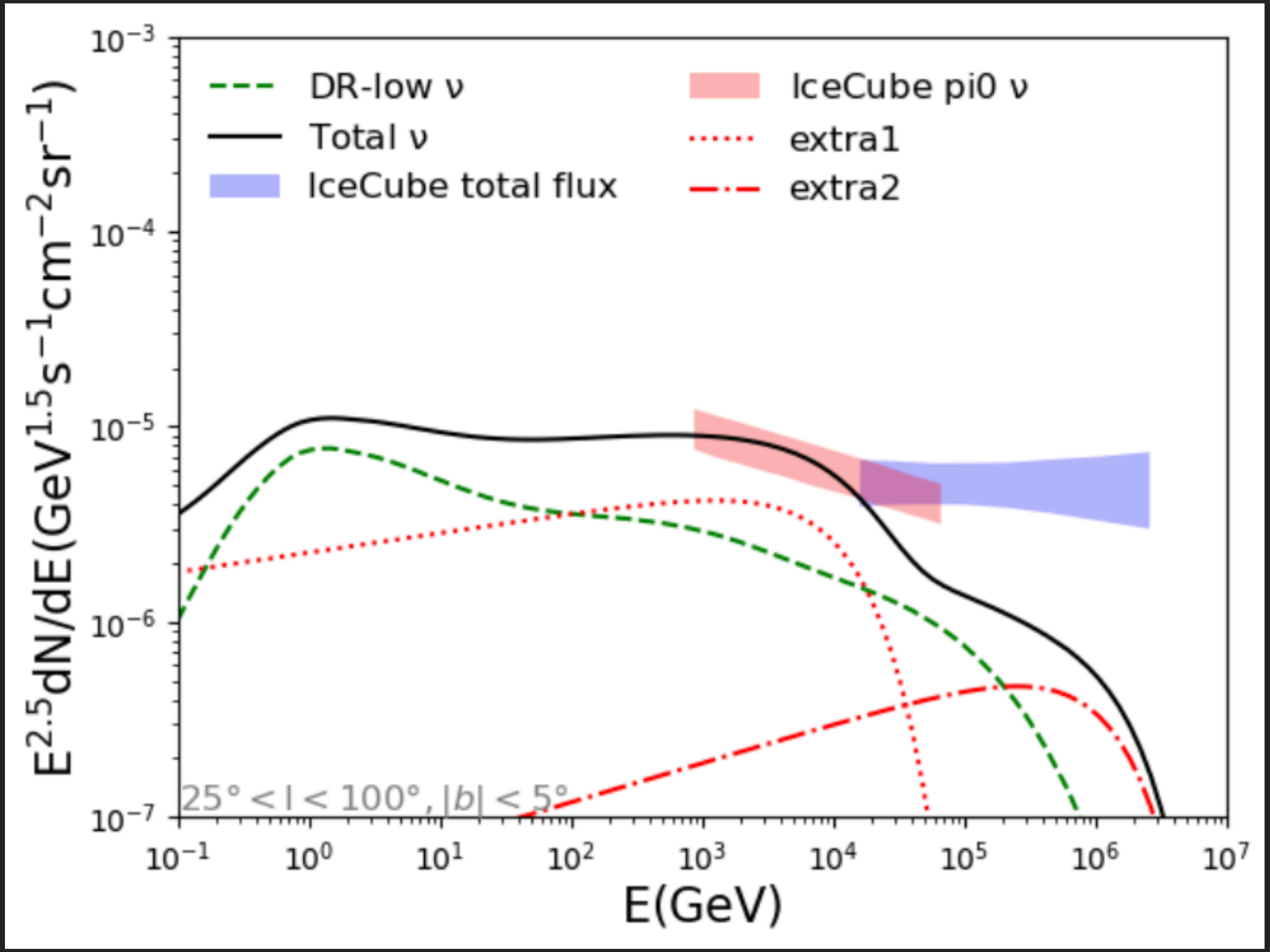

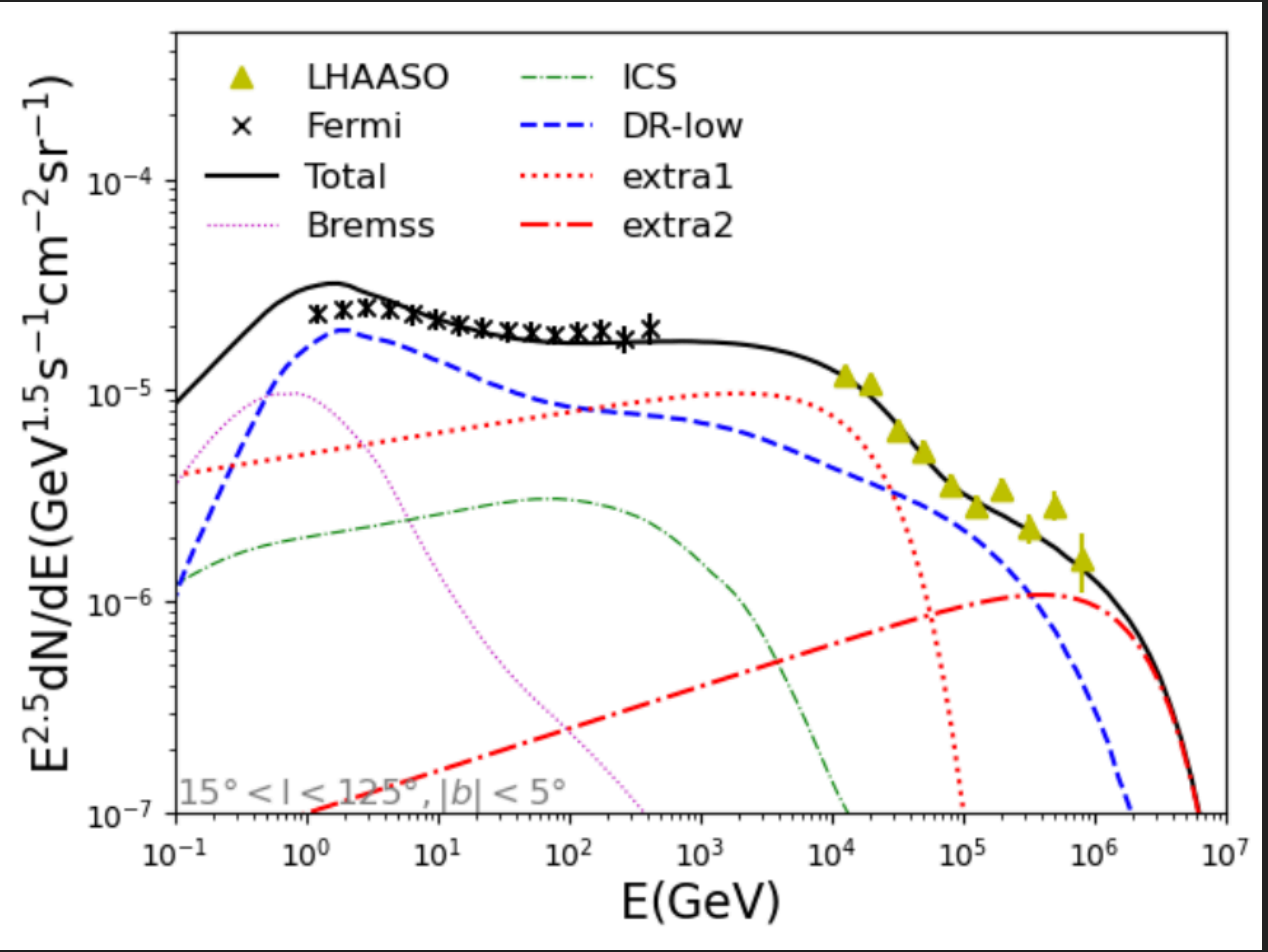

- Models that explain the IceCube neutrino flux still require an additional gamma-ray component (here: "Extra1 and Extra2") to produce the gamma-ray data from LHAASO.

THE TEV HALO ITSELF - DIFFERENCES IN DEFINITION

- An alternative definition of a "TeV halo" is used by Giacinti et al. 2019 (1907.12121)

- Linden et al. (2017) - A TeV halo is a leptonic gamma-ray source surrounding a pulsar, where the electrons are diffusing through the medium (rather than being driven by convective pulsar winds).

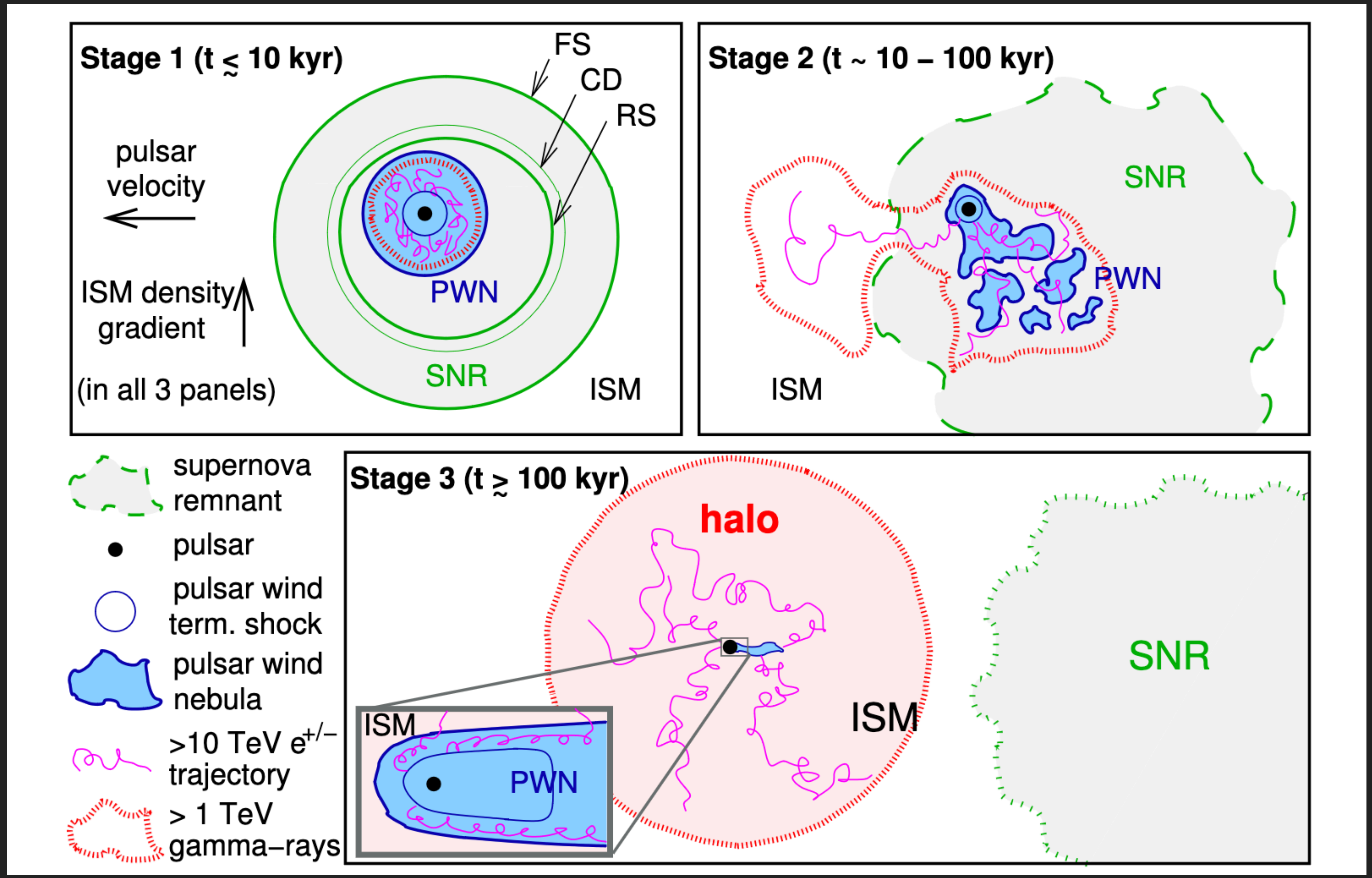

- Giacinti et al. (2019) - A TeV halo is a leptonic gamma-ray source surrounding a pulsar, where the emission stems from a region where the electron density falls below the ambient ISM electron density.

ADOPTING A MAXIMALIST VERSION OF TEV HALOS - OBSERVATIONS

Di Mauro, Manconi, Donato (2019; 1908.03216)

- In particular, this extended diffusive halos have been found in a number of young systems.
- Inhibited diffusion appears to occur very soon after system formation, and persist for a long time.

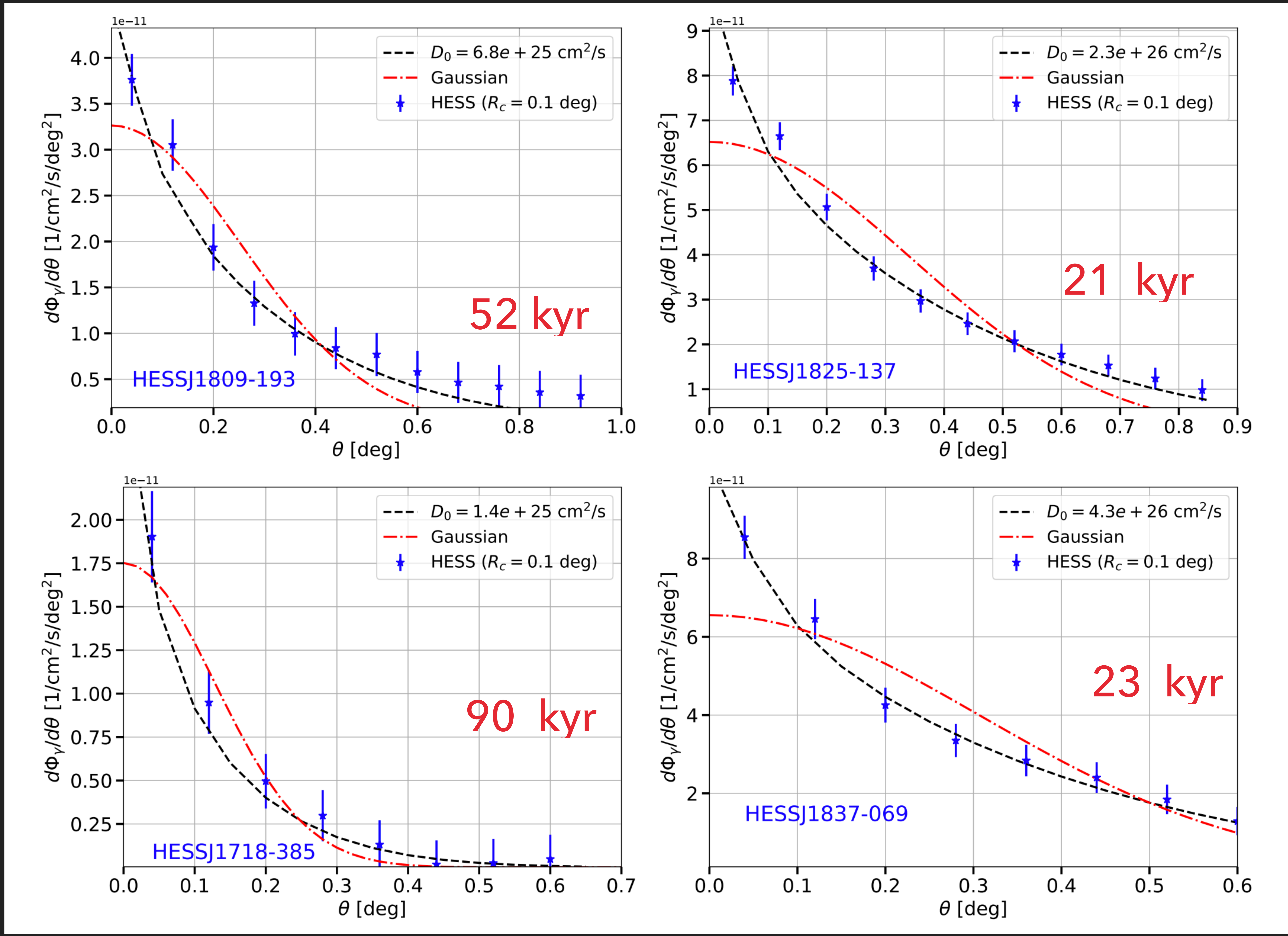

ADOPTING A MAXIMALIST VERSION OF TEV HALOS - OBSERVATIONS

Sudoh, Linden, Hooper (2101.11026)

- 8 out of the 9 HAWC sources observed above 56 TeV are consistent with the location of young pulsars.

- Likely PWN or composite objects – but TeV halo contributions must be carefully examined.

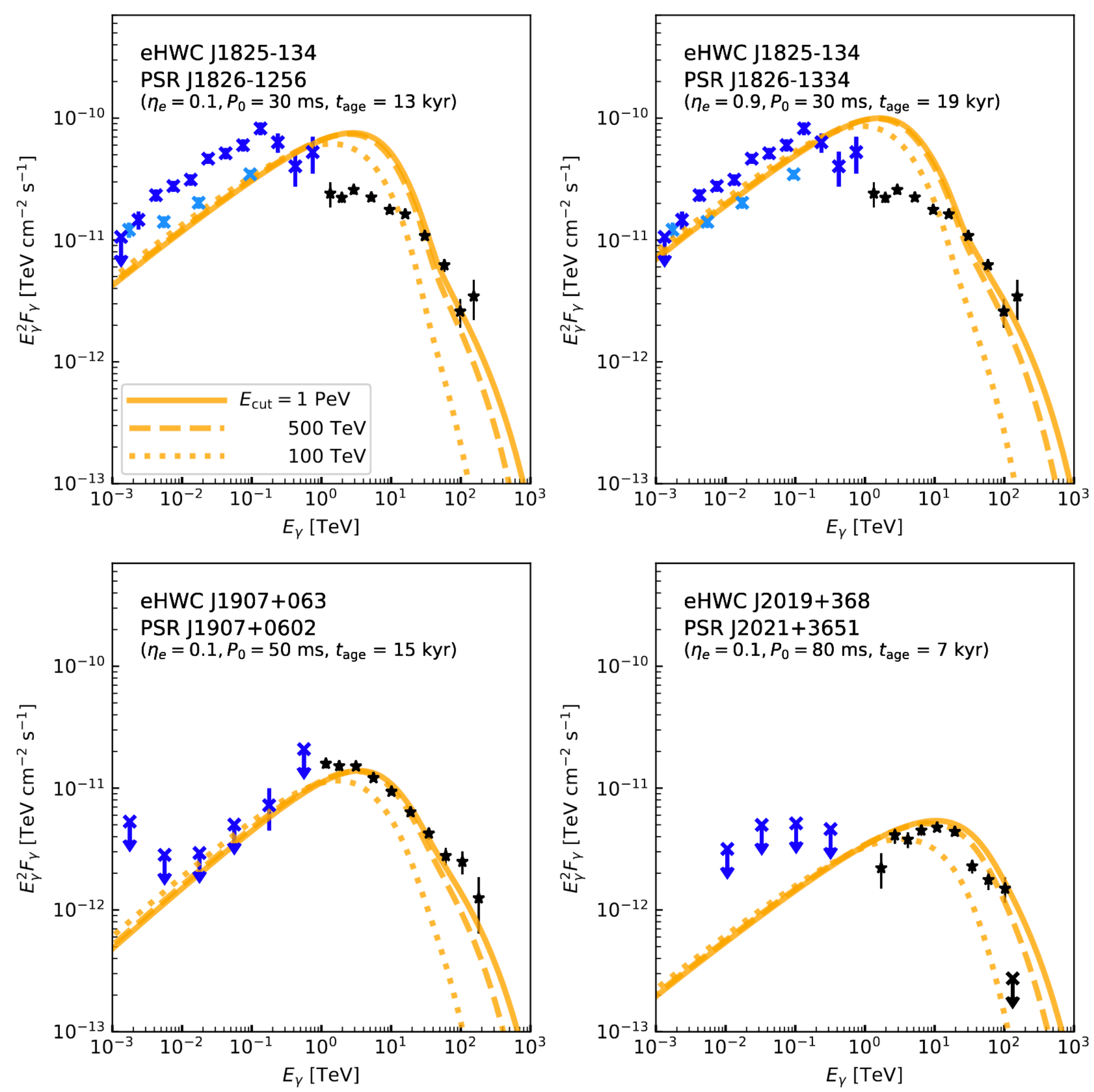

ADOPTING A MAXIMALIST VERSION OF TEV HALOS - OBSERVATIONS

- TeV Halos (Observationally):
  - Detected by all instruments (HAWC, LHAASO, HESS, VERITAS)
  - Currently just the tip of the Iceberg: Detected systems are nearby, or have high spin down power.

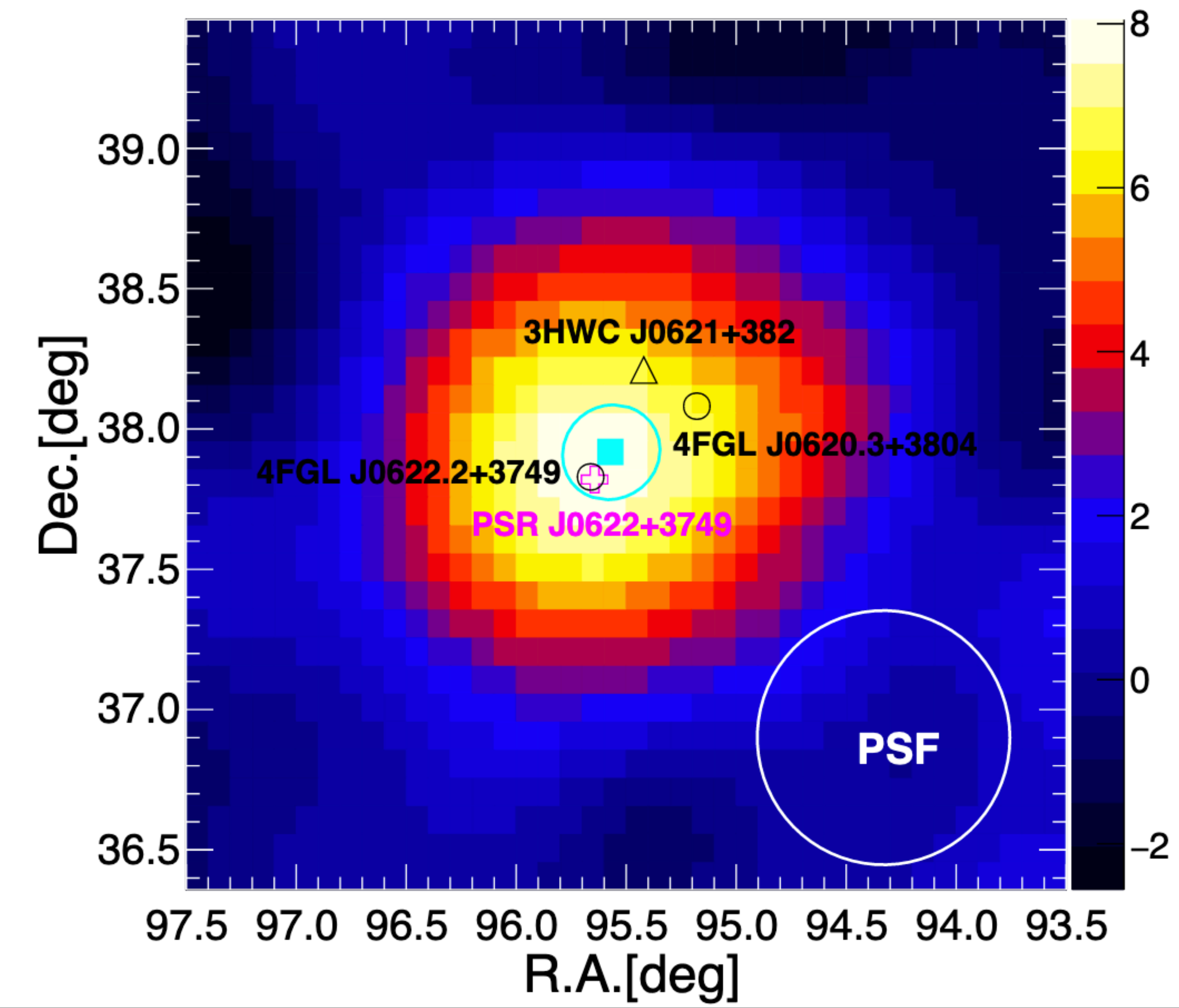

ATNF Name	Dec. (°)	Distance (kpc)	Age (kyr)	Spindown Lum. (erg s^{-1})	Spindown Flux (erg s^{-1} kpc^{-2})	2HWC
J0633+1746	17.77	0.25	342	3.2e34	4.1e34	2HWC J0631+169
B0656+14	14.23	0.29	111	3.8e34	3.6e34	2HWC J0700+143
B1951+32	32.87	3.00	107	3.7e36	3.3e34	—
J1740+1000	10.00	1.23	114	2.3e35	1.2e34	—
J1913+1011	10.18	4.61	169	2.9e36	1.1e34	2HWC J1912+099
J1831-0952	-9.86	3.68	128	1.1e36	6.4e33	2HWC J1831-098
J2032+4127	41.45	1.70	181	1.7e35	4.7e33	2HWC J2031+415
B1822-09	-9.58	0.30	232	4.6e33	4.1e33	—
B1830-08	-8.45	4.50	147	5.8e35	2.3e33	—
J1913+0904	9.07	3.00	147	1.6e35	1.4e33	—
B0540+23	23.48	1.56	253	4.1e34	1.4e33	—

ADOPTING A MAXIMALIST VERSION OF TEV HALOS - OBSERVATIONS

- "Mirage" sources
  - Anisotropic diffusion can produce sources that have extremely long tails.
  - Offset from pulsar position
- Can be difficult to detect and categorize, or associate with a known pulsar.

Tentative evidence of "Mirage" sources in LHAASO catalogs!

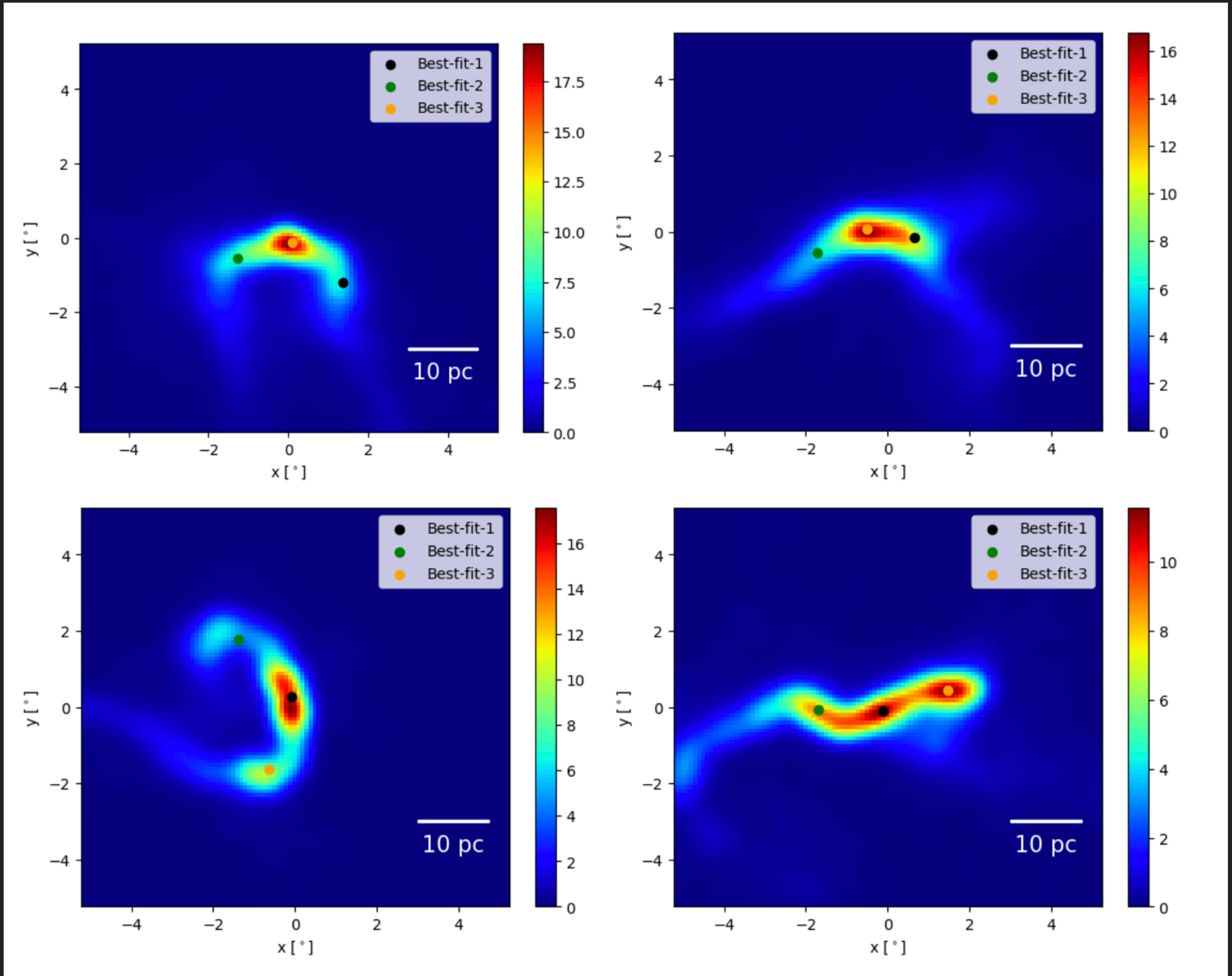

Stacking Searches for TeV Halos around Middle-aged and Millisecond Pulsars with HAWC

Hongyi Wu, Sara Coutiño de León, Ke Fang
University of Wisconsin - Madison

1

Chicago 2024

2024/8/25

UNDERSTANDING DIFFUSION IN TEV HALOS

- By combining the large number of TeV halo observations along with energetic considerations – we know that local diffusion must be inhibited.

Liu, Yan, Zhang (2019; 1904.11536)

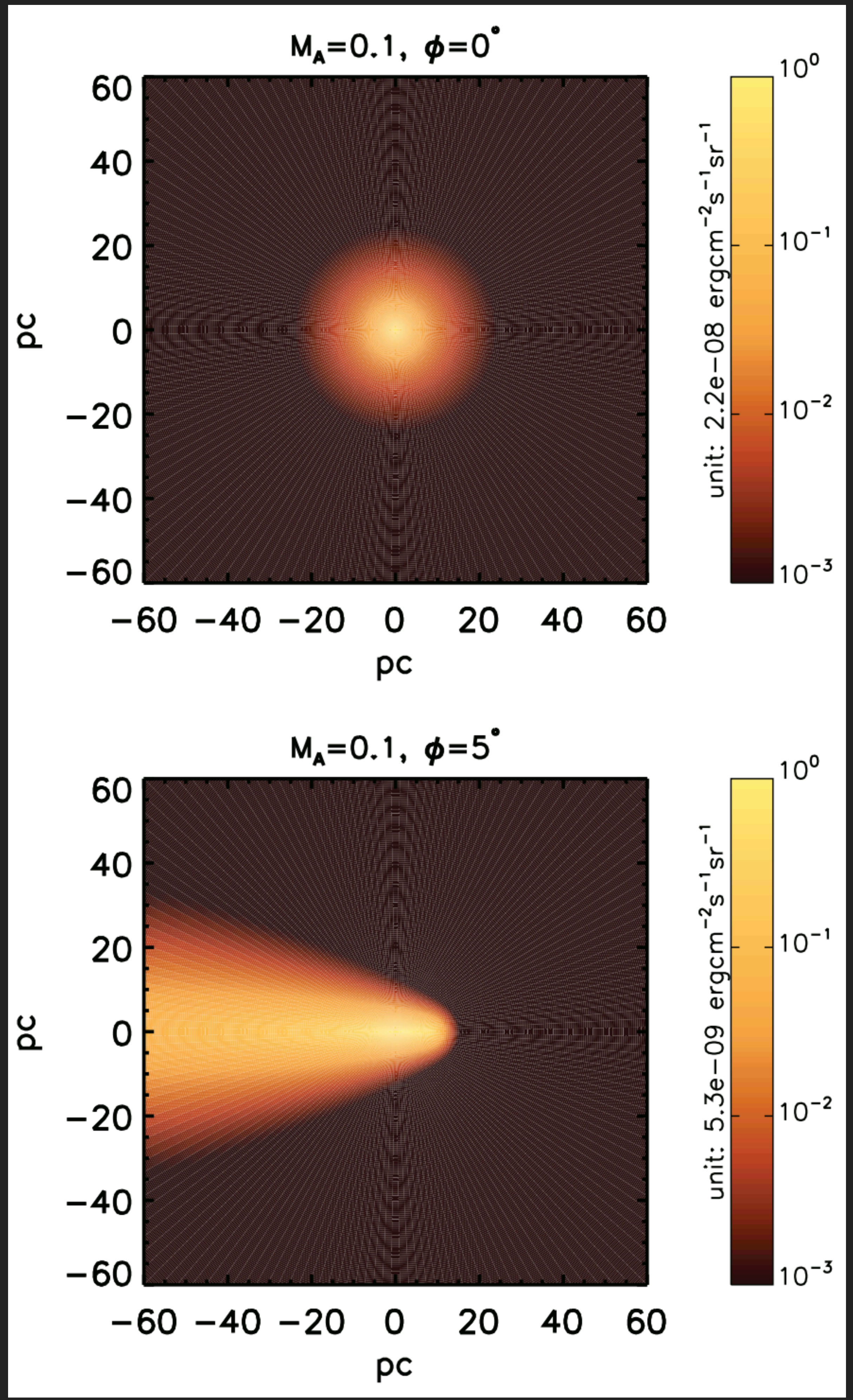

De la Torre Luque et al. (2022; 2205.08544)

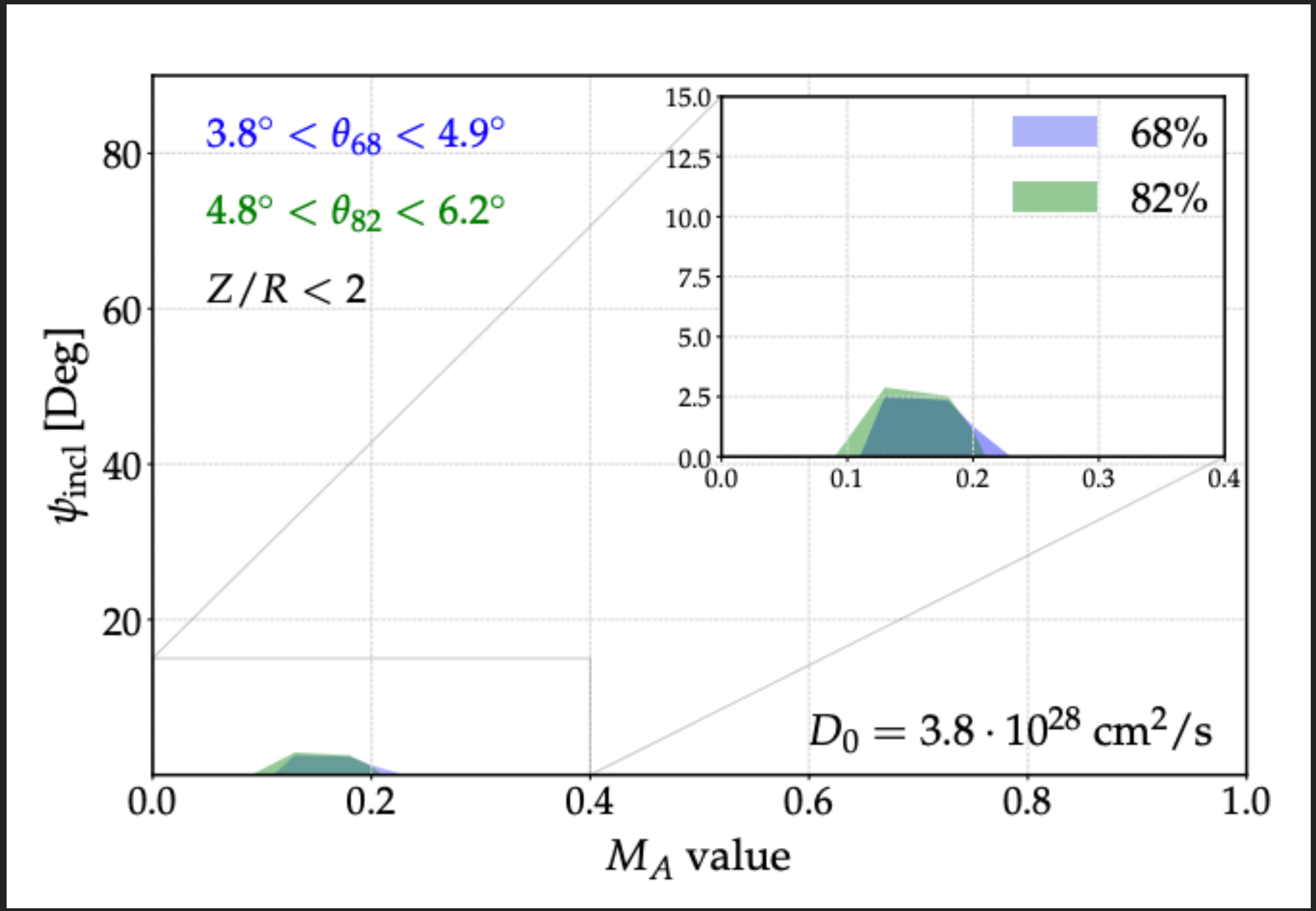

UNDERSTANDING DIFFUSION IN TEV HALOS

- By combining the large number of TeV halo observations along with energetic considerations – we know that local diffusion must be inhibited.

Recchia et al. (2021; 2106.02275)

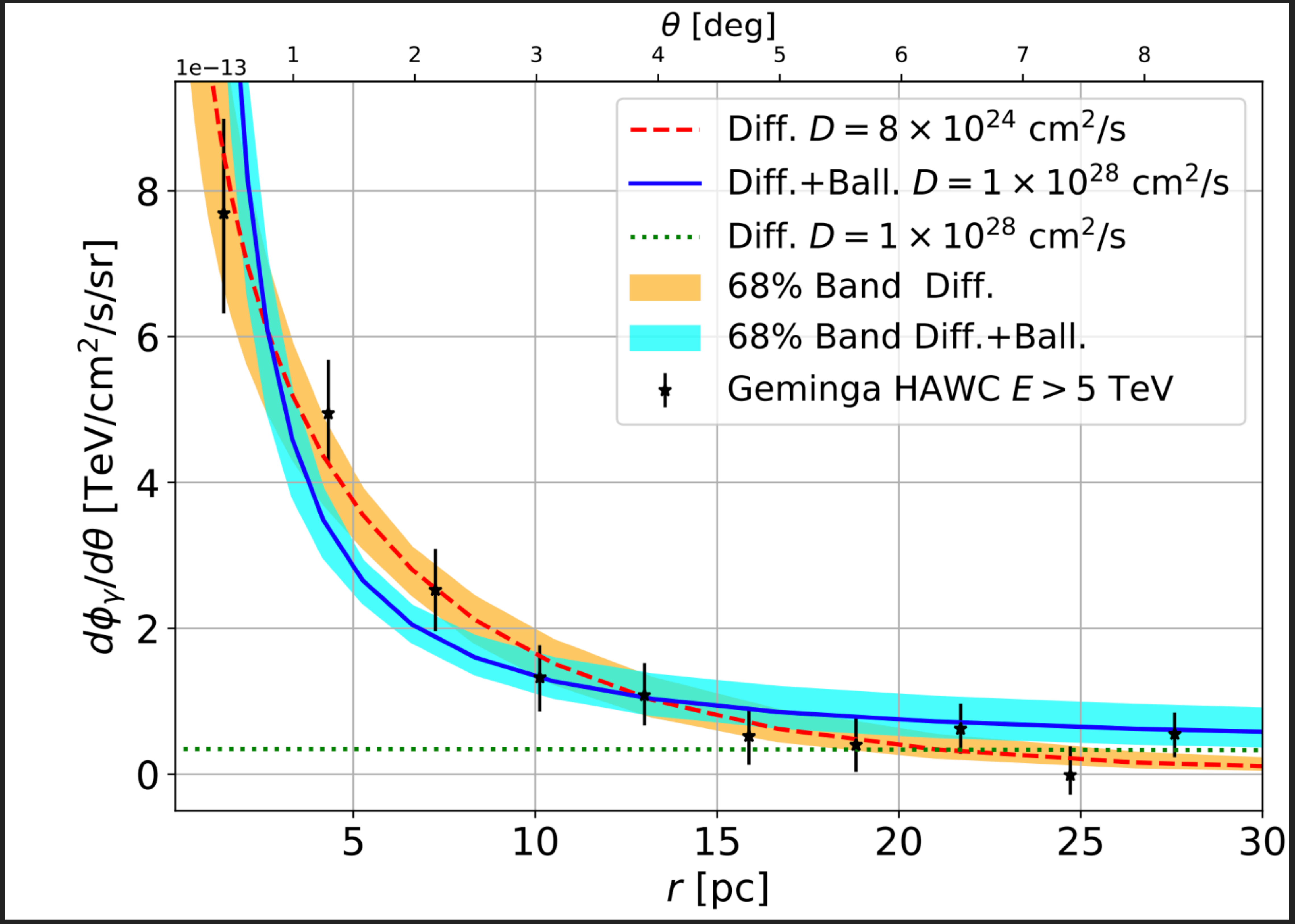

Bao et al. (2021; 2107.07395)

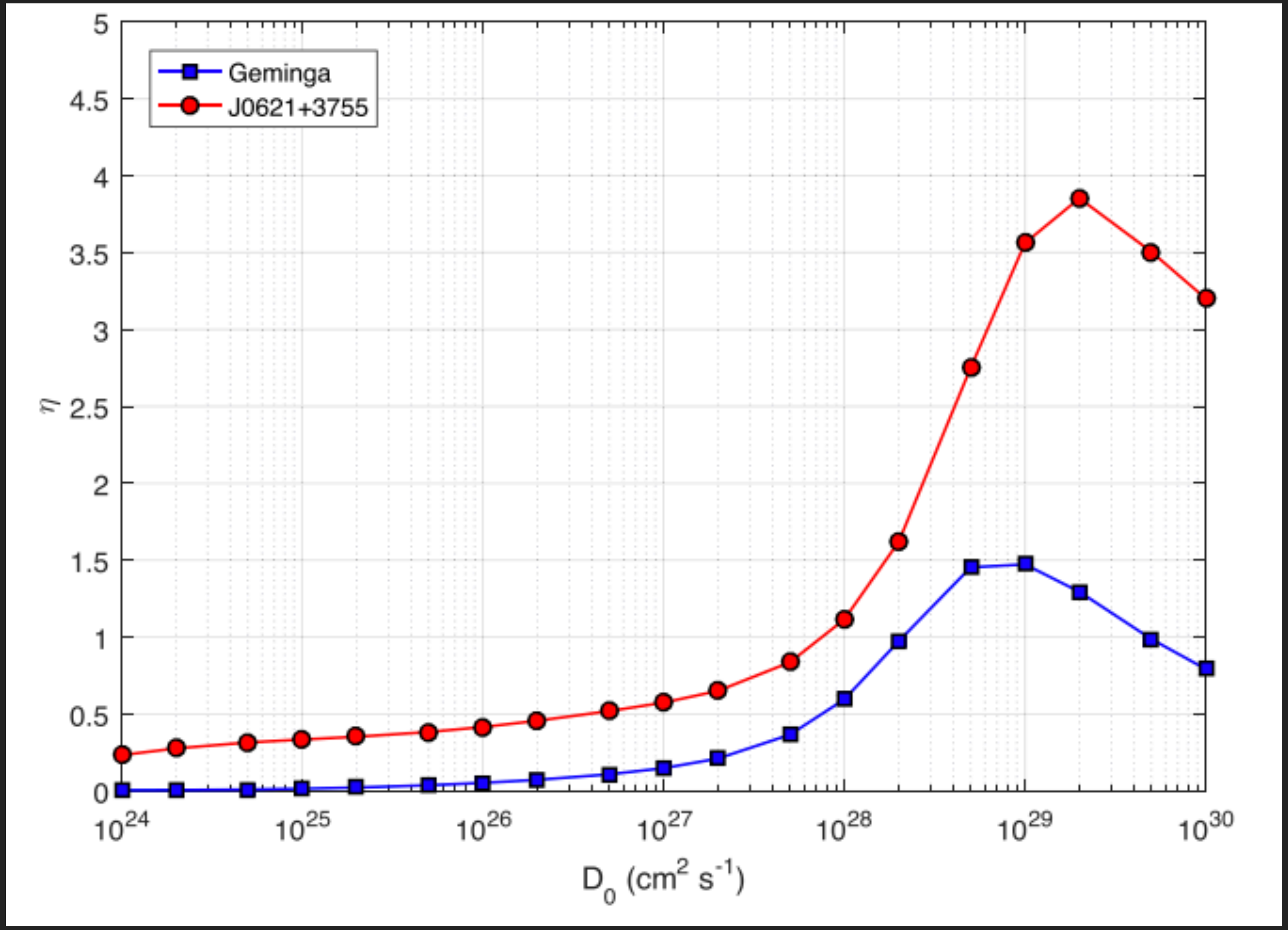

A PHYSICAL MODEL FOR TEV HALOS - MAXIMIZING IMPLICATIONS

- Self-confinement models (and most other models for inhibited diffusion) - require the high energy of a very young pulsar.

- Probing the diffusion around the youngest systems is critical for understanding TeV halo dynamics.

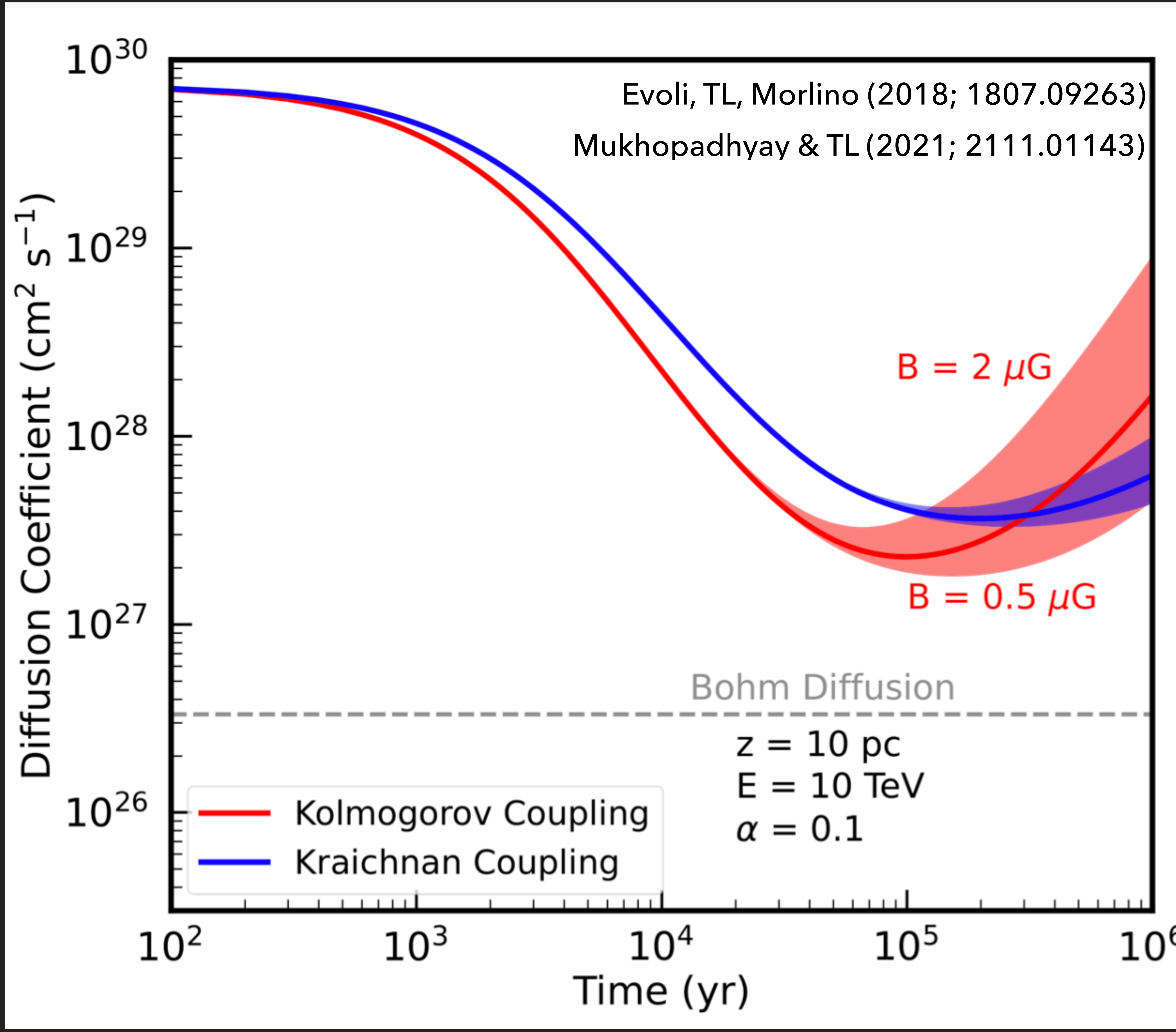

A PHYSICAL MODEL FOR TEV HALOS - MAXIMIZING IMPLICATIONS

Evoli, TL, Morlino (2018; 1807.09263)
Mukhopadhyay & TL (2021; 2111.01143)

$$\frac{\partial W}{\partial t} + v_A \frac{\partial W}{\partial z} = (\Gamma_{CR} + \Gamma_{NLD})\, W(k, z, t)$$

$$\Gamma_{CR}(k) = \frac{2\pi}{3} \frac{c\,|v_\alpha|}{k\;W(k)} \left(\frac{B_0^2}{8\pi}\right)^{-1} \left[p^4 \frac{\partial f}{\partial z}\right]_{p_{\rm res}}$$

$$\Gamma_{NLD}(k) = c_k\, v_\alpha \begin{cases} k^{3/2} W^{1/2} & \text{Kolmogorov} \\ k^2 W & \text{Kraichnan} \end{cases}$$

$$D(p, t) = \frac{4}{3\pi} \frac{c r_L(p))}{k_{\rm res} W(z, k_{\rm res}))}$$

- Many uncertainties in these models:
  - Role of Supernova Remnant
  - Disruption by molecular gas or magnetic fields
  - Pulsar Proper Motion
  - 1D vs. 3D diffusion
  - non-Resonant Terms
  - Halos in close proximity

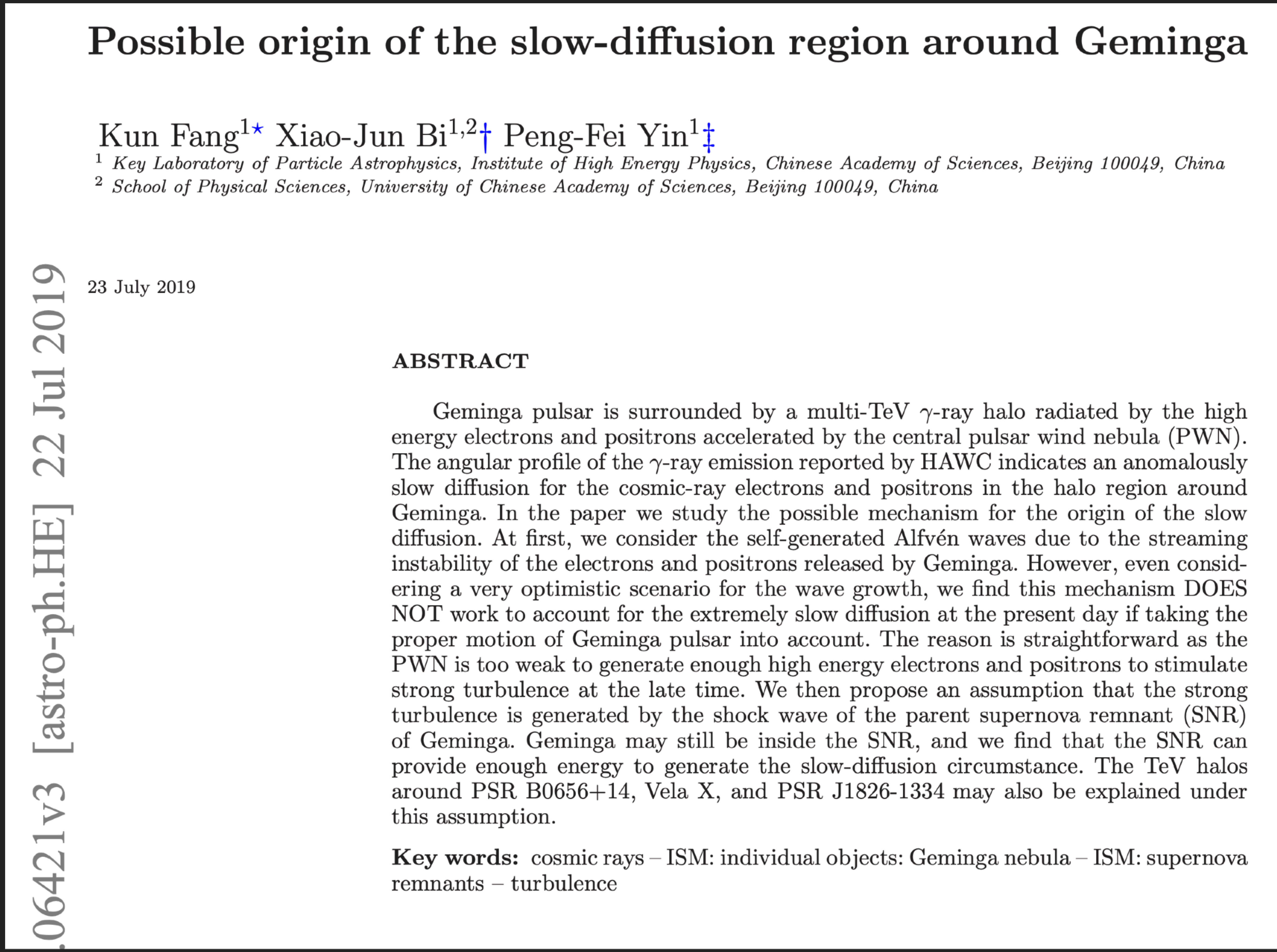

.06421v3 [astro-ph.HE] 22 Jul 2019

Possible origin of the slow-diffusion region around Geminga

Kun Fang[1⋆] Xiao-Jun Bi[1,2†] Peng-Fei Yin[1‡]
[1] *Key Laboratory of Particle Astrophysics, Institute of High Energy Physics, Chinese Academy of Sciences, Beijing 100049, China*
[2] *School of Physical Sciences, University of Chinese Academy of Sciences, Beijing 100049, China*

23 July 2019

ABSTRACT

Geminga pulsar is surrounded by a multi-TeV γ-ray halo radiated by the high energy electrons and positrons accelerated by the central pulsar wind nebula (PWN). The angular profile of the γ-ray emission reported by HAWC indicates an anomalously slow diffusion for the cosmic-ray electrons and positrons in the halo region around Geminga. In the paper we study the possible mechanism for the origin of the slow diffusion. At first, we consider the self-generated Alfvén waves due to the streaming instability of the electrons and positrons released by Geminga. However, even considering a very optimistic scenario for the wave growth, we find this mechanism DOES NOT work to account for the extremely slow diffusion at the present day if taking the proper motion of Geminga pulsar into account. The reason is straightforward as the PWN is too weak to generate enough high energy electrons and positrons to stimulate strong turbulence at the late time. We then propose an assumption that the strong turbulence is generated by the shock wave of the parent supernova remnant (SNR) of Geminga. Geminga may still be inside the SNR, and we find that the SNR can provide enough energy to generate the slow-diffusion circumstance. The TeV halos around PSR B0656+14, Vela X, and PSR J1826-1334 may also be explained under this assumption.

Key words: cosmic rays – ISM: individual objects: Geminga nebula – ISM: supernova remnants – turbulence

A PHYSICAL MODEL FOR TEV HALOS - MAXIMIZING IMPLICATIONS

Evoli, TL, Morlino (2018; 1807.09263)

Mukhopadhyay & TL (2021; 2111.01143)

- Many uncertainties in these models:
  - Role of Supernova Remnant
  - Disruption by molecular gas or magnetic fields
  - Pulsar Proper Motion
  - 1D vs. 3D diffusion
  - non-Resonant Terms
  - Halos in close proximity

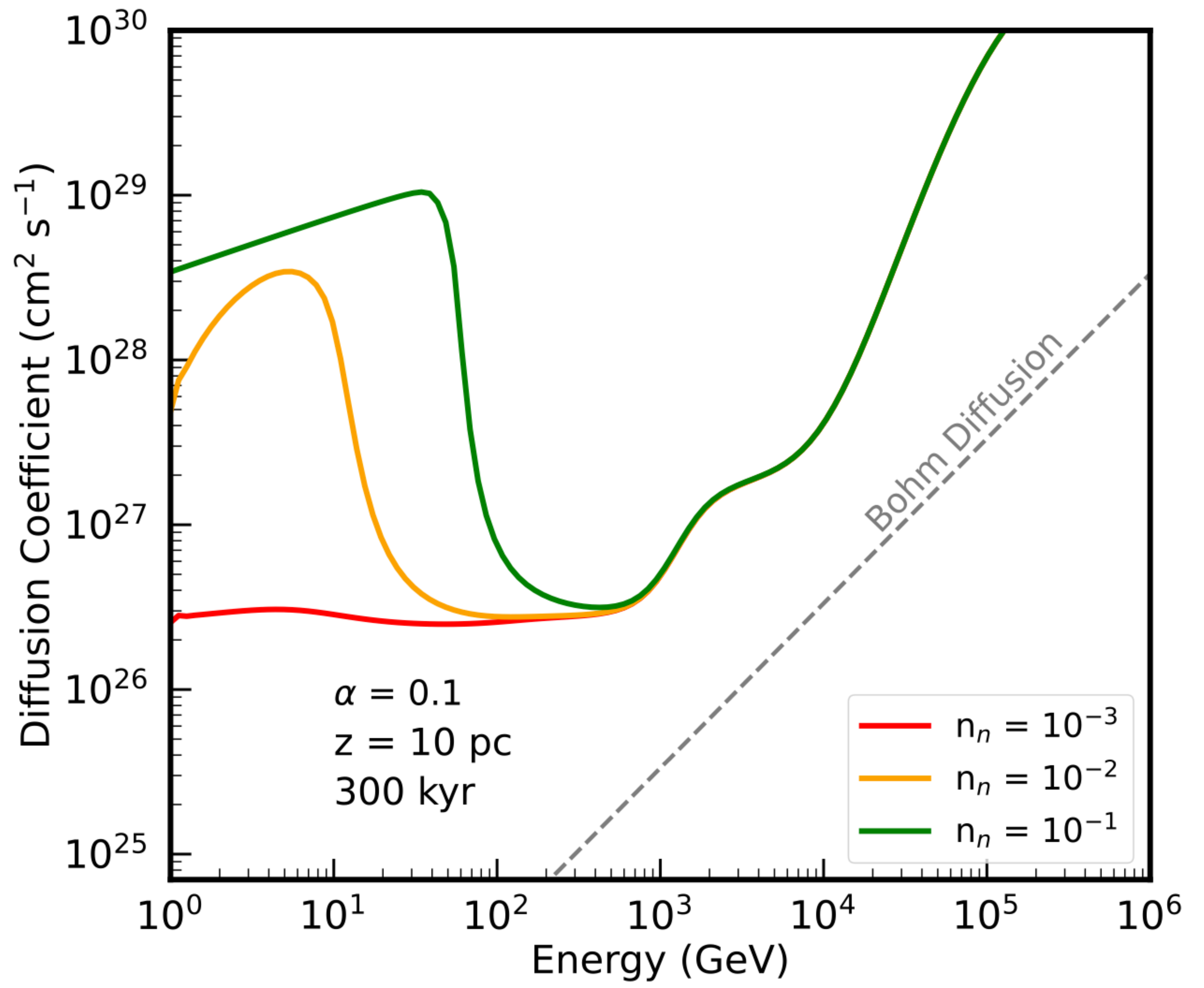

Evoli, TL, Morlino (2018; 1807.09263)
Mukhopadhyay & TL (2021; 2111.01143)

TEV HALOS SOLVE COSMIC-RAY DIFFUSION

- Many uncertainties in these models:
  - Role of Supernova Remnant
  - Disruption by molecular gas or magnetic fields
  - Pulsar Proper Motion
  - 1D vs. 3D diffusion
  - non-Resonant Terms
  - Halos in close proximity

?

TEV HALOS SOLVE COSMIC-RAY DIFFUSION

Mukhopadhyay & TL (2021; 2111.01143)

- Many uncertainties in these models:
  - Role of Supernova Remnant
  - Disruption by molecular gas or magnetic fields
  - Pulsar Proper Motion
  - 1D vs. 3D diffusion
  - non-Resonant Terms
  - Halos in close proximity

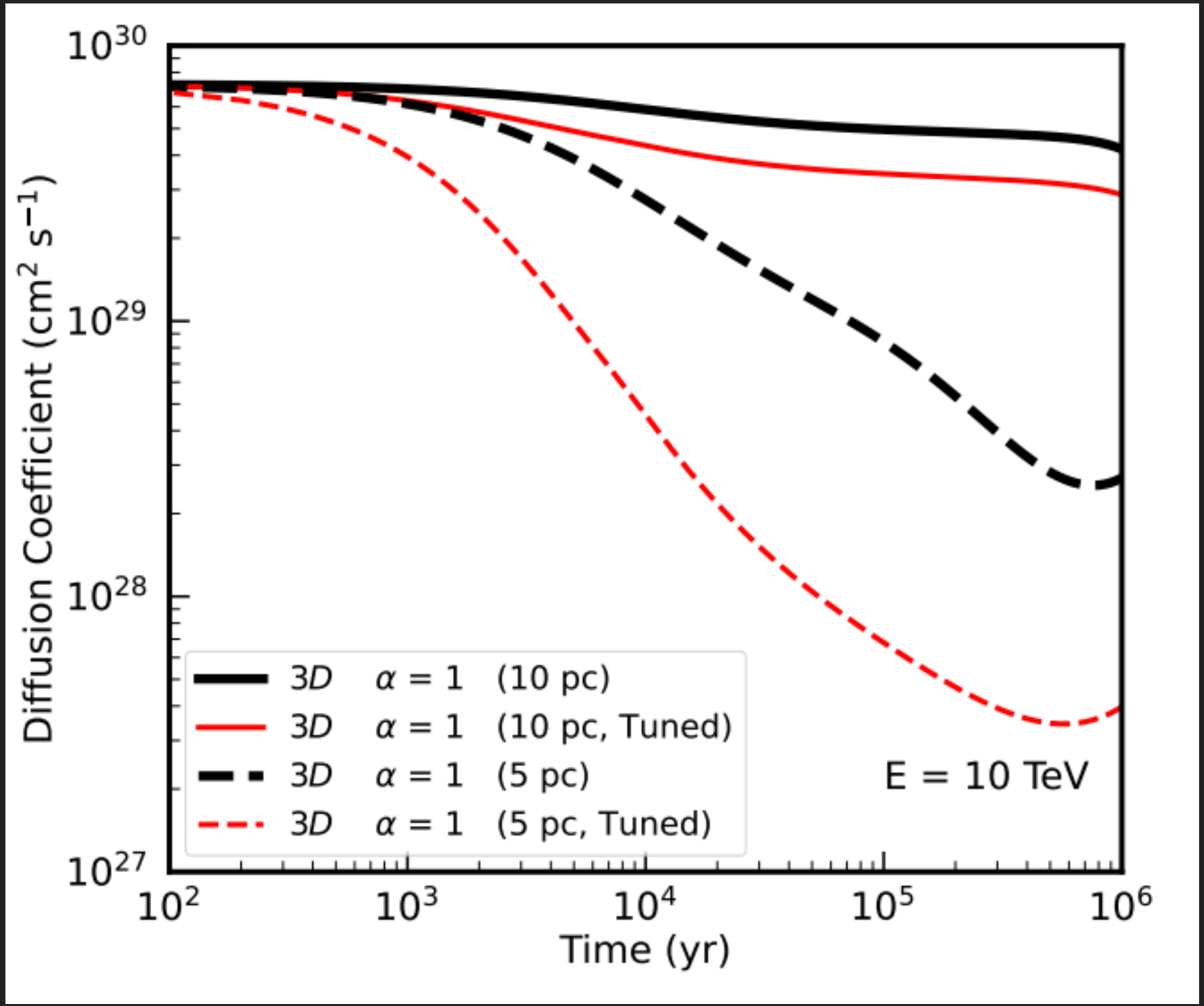

TEV HALOS SOLVE COSMIC-RAY DIFFUSION

Evoli, TL, Morlino (2018; 1807.09263)
Mukhopadhyay & TL (2021; 2111.01143)

- Many uncertainties in these models:
  - Role of Supernova Remnant
  - Disruption by molecular gas or magnetic fields
  - Pulsar Proper Motion
  - 1D vs. 3D diffusion
  - non-Resonant Terms
  - Halos in close proximity

?

TEV HALOS SOLVE COSMIC-RAY DIFFUSION

Evoli, TL, Morlino (2018; 1807.09263)
Mukhopadhyay & TL (2021; 2111.01143)

- Many uncertainties in these models:
  - Role of Supernova Remnant
  - Disruption by molecular gas or magnetic fields
  - Pulsar Proper Motion
  - 1D vs. 3D diffusion
  - non-Resonant Terms
  - Halos in close proximity

?

TEV HALOS SOLVE COSMIC-RAY DIFFUSION

Evoli, TL, Morlino (2018; 1807.09263)
Mukhopadhyay & TL (2021; 2111.01143)

- Several Predictions of these Models:
  - Relatively flat low-energy diffusion coefficient.
  - Highly energy dependent diffusion coefficient at high energies.

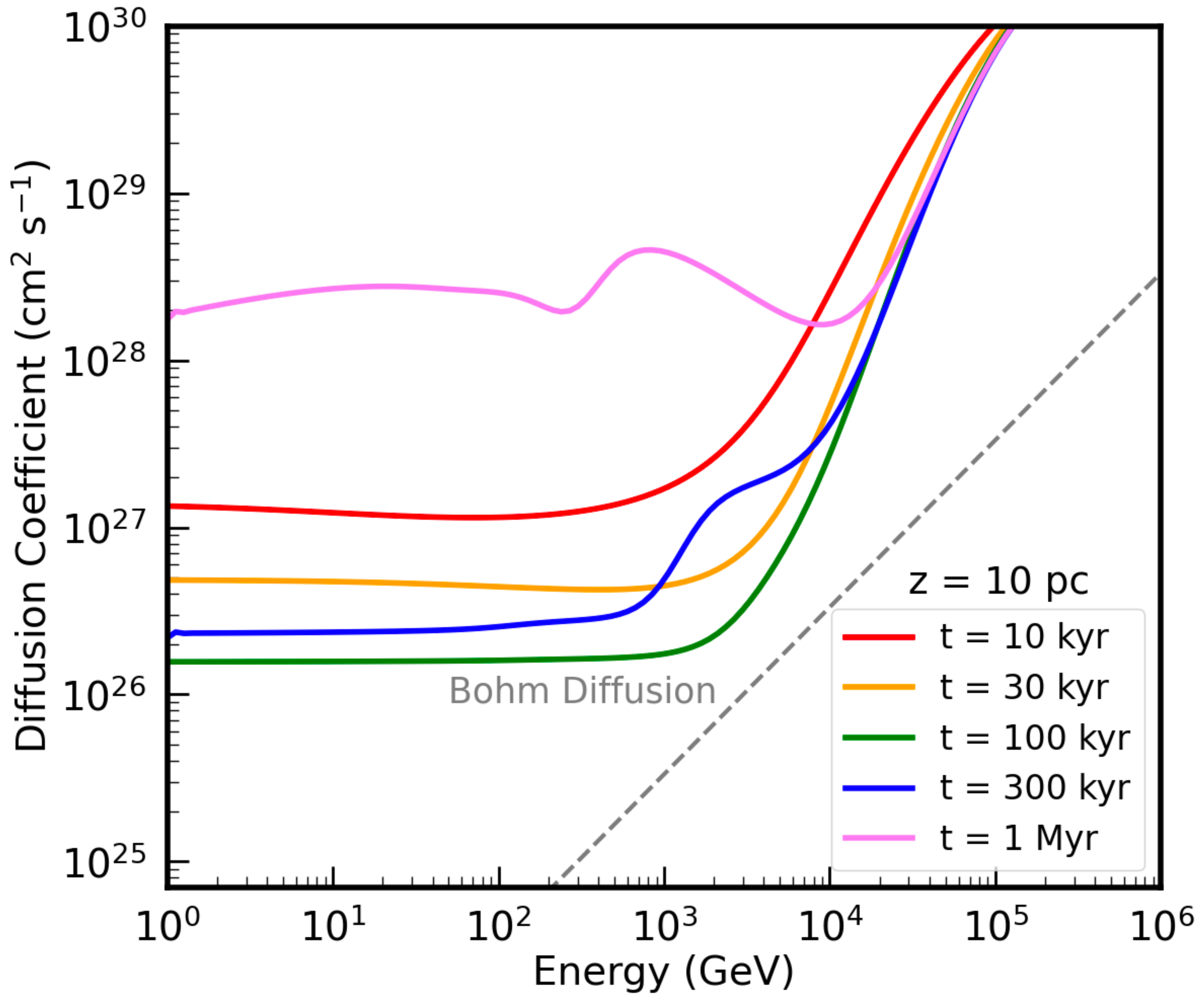

Kinetic simulations of electron-positron induced streaming instability in the context of gamma-ray halos around pulsars

Illya Plotnikov [1], Allard Jan van Marle [2], Claire Guépin [2], Alexandre Marcowith [2], and Pierrick Martin [1]

[1] IRAP, CNRS, OMP, Université de Toulouse III – Paul Sabatier, Toulouse, France
e-mail: illya.plotnikov@irap.omp.eu
[2] Laboratoire Univers et Particules de Montpellier (LUPM), Université de Montpellier, CNRS/IN2P3, CC72, Place Eugène Bataillon, F-34095 Montpellier Cedex 5, France

Received Month XX, 2024; accepted Month XX, 2024

ABSTRACT

Context. The possibility of slow diffusion regions as the origin for extended TeV emission halos around some pulsars (such as PSR J0633+1746 and PSR B0656+14) challenges the standard scaling of the electron diffusion coefficient in the interstellar medium.
Aims. Self-generated turbulence by electron-positron pairs streaming out of the pulsar wind nebula was proposed as a possible mechanism to produce the enhanced turbulence required to explain the morphology and brightness of these TeV halos.
Methods. We perform fully kinetic 1D3V particle-in-cell simulations of this instability, considering the case where streaming electrons and positrons have the same density. This implies purely resonant instability as the beam does not carry any current.
Results. We compare the linear phase of the instability with analytical theory and find very reasonable agreement. The non-linear phase of the instability is also studied, which reveals that the intensity of saturated waves is consistent with a momentum exchange criterion between a decelerating beam and growing magnetic waves. With the adopted parameters, the instability-driven wavemodes cover both the Alfvénic (fluid) and kinetic scales. The spectrum of the produced waves is non-symmetric, with left-handed circular polarisation waves being strongly damped when entering the ion-cyclotron branch, while right-handed waves are suppressed at smaller wavelength when entering the Whistler branch. The low-wavenumber part of the spectrum remains symmetric when in the Alfvénic branch. As a result, positrons behave dynamically differently compared to electrons. The final drift velocity of positrons can maintain a larger value than the ambient Alfvén speed V_A while the drift of electrons can drop below V_A. We also observed a second harmonic plasma emission in the wave spectrum. An MHD-PIC approach is warranted to probe hotter beams and investigate the Alfvén branch physics. We provide a few such test simulations to support this assertion.
Conclusions. This work confirms that the self-confinement scenario develops essentially according to analytical expectations, but some of the adopted approximations (like the distribution of non-thermal particles in the beam) need to be revised and other complementary numerical techniques should be used to get closer to more realistic configuration.

Key words. Pulsars:general – Instabilities – Plasmas – Methods: numerical

CONFIRMATION FROM SIMULATIONS

Plotnikov et al. (2024; 2406.02945)

- Results in the linear regime are consistent between PIC simulations and analytic models
- In non-linear regime - several new effects
  - Difference between right-handed and left-handed waves in an ionic background causes positrons to propagate faster than electrons.

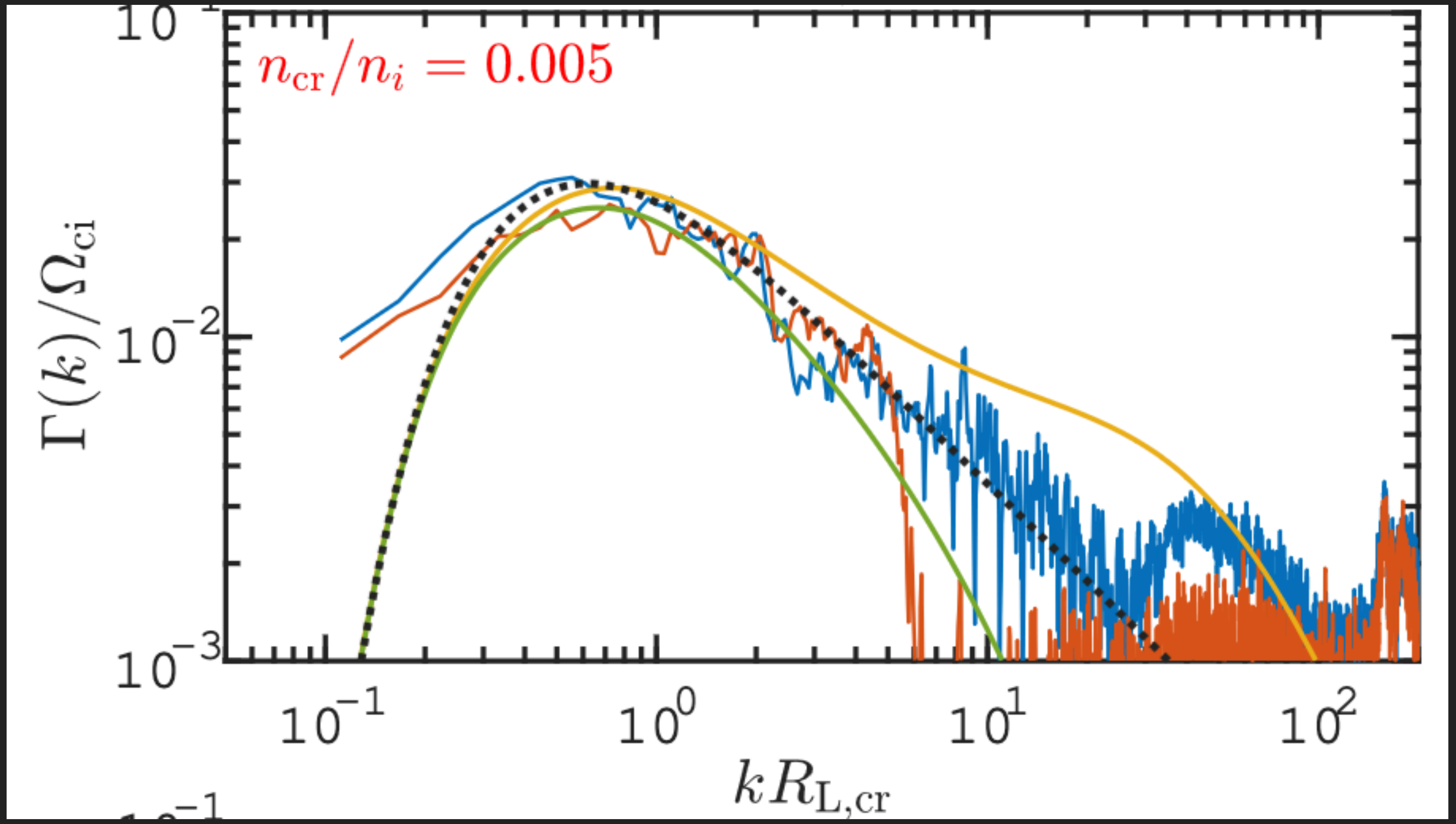

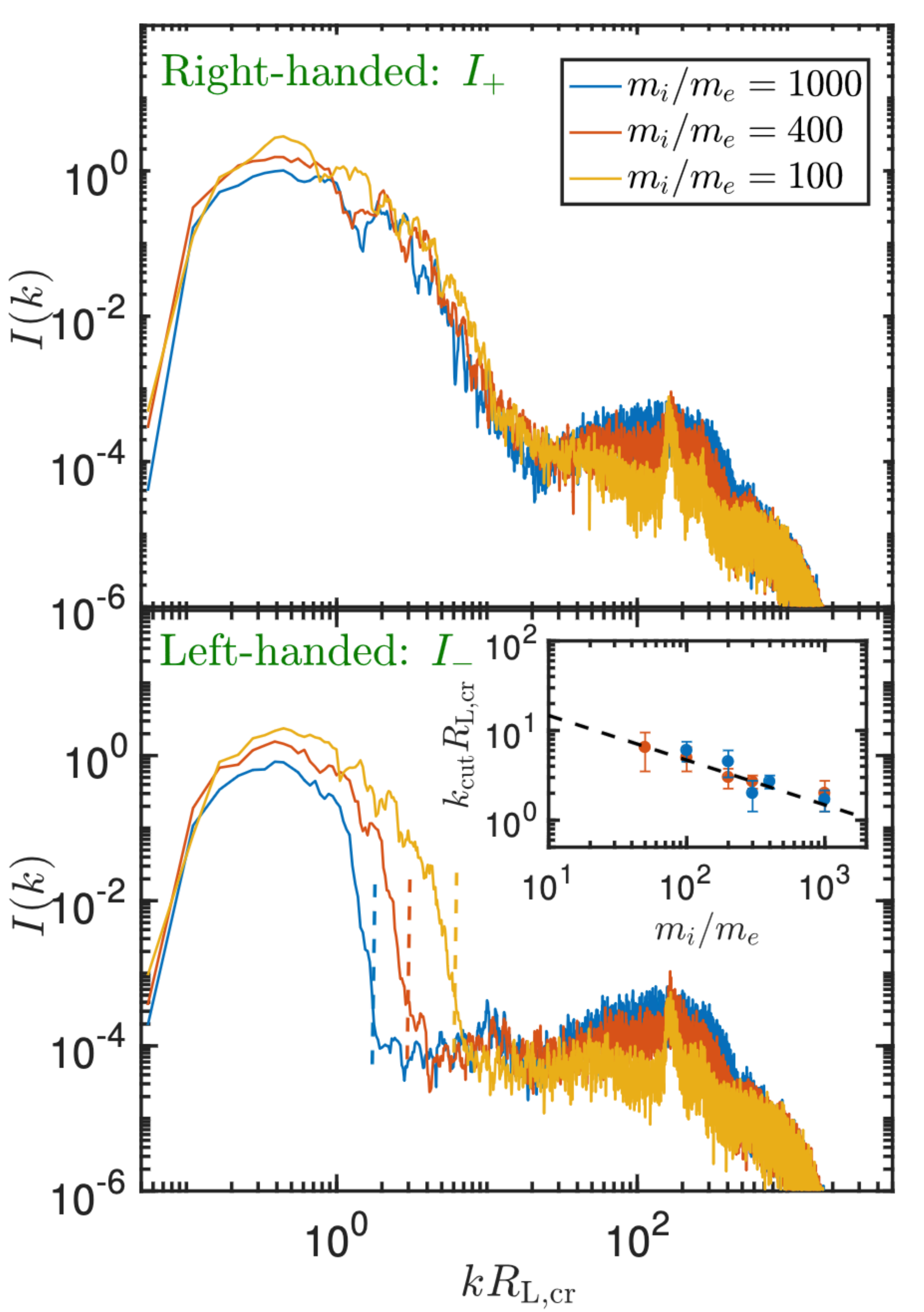

Kinetic simulations of electron-positron induced streaming instability in the context of gamma-ray halos around pulsars

Illya Plotnikov [1], Allard Jan van Marle [2], Claire Guépin [2], Alexandre Marcowith [2], and Pierrick Martin [1]

[1] IRAP, CNRS, OMP, Université de Toulouse III – Paul Sabatier, Toulouse, France
e-mail: illya.plotnikov@irap.omp.eu
[2] Laboratoire Univers et Particules de Montpellier (LUPM), Université de Montpellier, CNRS/IN2P3, CC72, Place Eugène Bataillon, F-34095 Montpellier Cedex 5, France

Received Month XX, 2024; accepted Month XX, 2024

ABSTRACT

Context. The possibility of slow diffusion regions as the origin for extended TeV emission halos around some pulsars (such as PSR J0633+1746 and PSR B0656+14) challenges the standard scaling of the electron diffusion coefficient in the interstellar medium.
Aims. Self-generated turbulence by electron-positron pairs streaming out of the pulsar wind nebula was proposed as a possible mechanism to produce the enhanced turbulence required to explain the morphology and brightness of these TeV halos.
Methods. We perform fully kinetic 1D3V particle-in-cell simulations of this instability, considering the case where streaming electrons and positrons have the same density. This implies purely resonant instability as the beam does not carry any current.
Results. We compare the linear phase of the instability with analytical theory and find very reasonable agreement. The non-linear phase of the instability is also studied, which reveals that the intensity of saturated waves is consistent with a momentum exchange criterion between a decelerating beam and growing magnetic waves. With the adopted parameters, the instability-driven wavemodes cover both the Alfvénic (fluid) and kinetic scales. The spectrum of the produced waves is non-symmetric, with left-handed circular polarisation waves being strongly damped when entering the ion-cyclotron branch, while right-handed waves are suppressed at smaller wavelength when entering the Whistler branch. The low-wavenumber part of the spectrum remains symmetric when in the Alfvénic branch. As a result, positrons behave dynamically differently compared to electrons. The final drift velocity of positrons can maintain a larger value than the ambient Alfvén speed V_A while the drift of electrons can drop below V_A. We also observed a second harmonic plasma emission in the wave spectrum. An MHD-PIC approach is warranted to probe hotter beams and investigate the Alfvén branch physics. We provide a few such test simulations to support this assertion.
Conclusions. This work confirms that the self-confinement scenario develops essentially according to analytical expectations, but some of the adopted approximations (like the distribution of non-thermal particles in the beam) need to be revised and other complementary numerical techniques should be used to get closer to more realistic configuration.

Key words. Pulsars:general – Instabilities – Plasmas – Methods: numerical


VLZ 6000-00

THE FUTURE: THE PROMISE OF TEV HALOS FOR DIFFUSE EMISSION STUDIES

- High Angular Resolution

- Long energy-lever arm (20 GeV – 100 TeV)

- Bifurcation in electron/proton morphology
  - $D_{\mathrm{proton}} \propto E^{\delta/2}$
  - $D_{\mathrm{electron}} \propto E^{\delta/2-1}$

NEED MODELS IN ORDER TO USE THESE OBSERVATIONS TO UNDERSTAND PHYSICS

$$\overbrace{\frac{\partial\psi\left(\vec{r},p,t\right)}{\partial t}}^{\text{flux}} = \overbrace{Q\left(\vec{r},p,t\right)}^{\text{source}} + \vec{\nabla}\times\big(\overbrace{D_{xx}\vec{\nabla}\psi}^{\text{diffusion}} - \overbrace{\vec{V}\psi}^{\text{convection}}\big) + \overbrace{\frac{\partial}{\partial p}p^{2}D_{pp}\frac{\partial}{\partial p^{2}}\psi}^{\text{re-acceleration}}$$

$$-\underbrace{\frac{\partial}{\partial p}\left(\dot{p}\psi - \frac{p}{3}\left(\vec{\nabla}\times\vec{V}\right)\psi\right)}_{\text{energy loss}} - \underbrace{\frac{\psi}{\tau_f}}_{\text{fragmentation}} - \underbrace{\frac{\psi}{\tau_r}}_{\text{radioactive decay}}$$

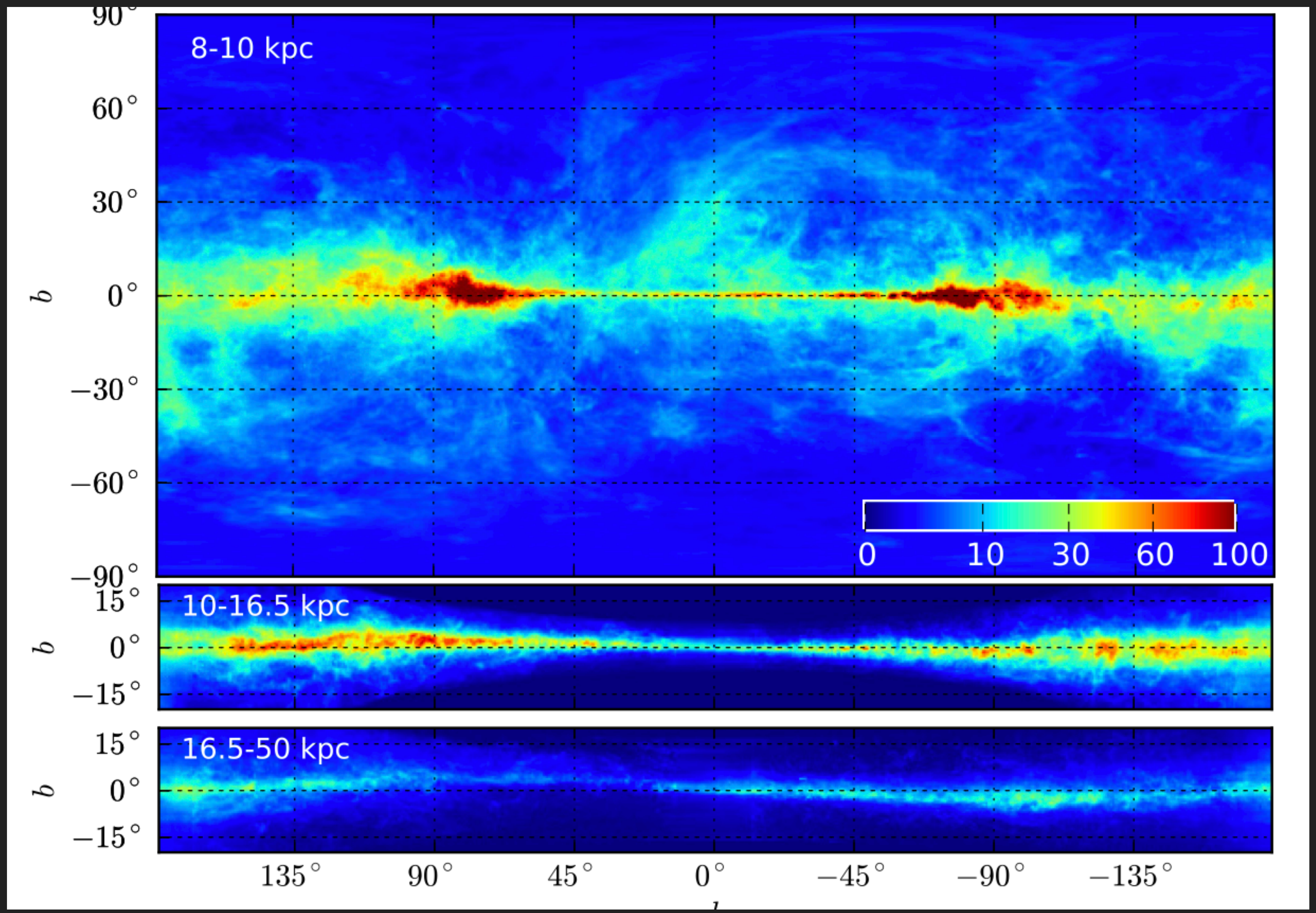

TEV HALOS BREAK GEV GAMMA-RAY DIFFUSE EMISSION MODELS

Korsmeier & Cuoco (2016; 1607.06093)

Fit parameters		(uni-PHe)	(uni-PHePbar)	(P)	(PHe)	(main)	(diMauro)	(1GV)	(noVc-1GV)	(noVc-5GV)
$\gamma_{1,p}$		-	-	$1.52^{+0.21}_{-0.32}$	$1.27^{+0.11}_{-0.07}$	$1.36^{+0.07}_{-0.10}$	$1.38^{+0.07}_{-0.10}$	$1.32^{+0.05}_{-0.12}$	$1.61^{+0.06}_{-0.10}$	$1.76^{+0.07}_{-0.04}$
$\gamma_{2,p}$		-	-	$2.52^{+0.12}_{-0.45}$	$2.069^{+0.098}_{-0.069}$	$2.493^{+0.010}_{-0.026}$	$2.499^{+0.026}_{-0.014}$	$2.455^{+0.014}_{-0.007}$	$2.421^{+0.010}_{-0.014}$	$2.454^{+0.026}_{-0.014}$
γ_1		$1.92^{+0.08}_{-0.14}$	$1.50^{+0.07}_{-0.12}$	-	$1.53^{+0.24}_{-0.11}$	$1.29^{+0.04}_{-0.09}$	$1.26^{+0.10}_{-0.06}$	$1.32^{+0.06}_{-0.12}$	$1.65^{+0.07}_{-0.11}$	$1.70^{+0.06}_{-0.07}$
γ_2		$2.582^{+0.010}_{-0.034}$	$2.404^{+0.006}_{-0.022}$	-	$2.003^{+0.094}_{-0.003}$	$2.440^{+0.006}_{-0.018}$	$2.451^{+0.018}_{-0.010}$	$2.412^{+0.012}_{-0.006}$	$2.381^{+0.010}_{-0.010}$	$2.407^{+0.022}_{-0.014}$
R_0	[GV]	$8.16^{+1.22}_{-1.54}$	$8.79^{+1.17}_{-1.55}$	$4.38^{+3.23}_{-1.54}$	$10.5^{+1.40}_{-1.59}$	$5.54^{+0.76}_{-0.54}$	$5.44^{+0.54}_{-0.54}$	$5.52^{+0.33}_{-0.83}$	$7.01^{+0.98}_{-0.54}$	$8.63^{+0.98}_{-0.76}$
s		$0.32^{+0.08}_{-0.02}$	$0.41^{+0.09}_{-0.07}$	$0.48^{+0.16}_{-0.31}$	$0.59^{+0.16}_{-0.04}$	$0.50^{+0.02}_{-0.04}$	$0.50^{+0.05}_{-0.03}$	$0.43^{+0.04}_{-0.03}$	$0.31^{+0.03}_{-0.03}$	$0.32^{+0.04}_{-0.05}$
δ		$0.16^{+0.03}_{-0.02}$	$0.36^{+0.04}_{-0.03}$	$0.29^{+0.46}_{-0.18}$	$0.72^{+0.01}_{-0.11}$	$0.28^{+0.03}_{-0.01}$	$0.27^{+0.02}_{-0.04}$	$0.32^{+0.03}_{-0.02}$	$0.40^{+0.01}_{-0.01}$	$0.36^{+0.02}_{-0.02}$
D_0	$[10^{28}\ \mathrm{cm^2/s}]$	$2.77^{+2.95}_{-0.53}$	$2.83^{+0.90}_{-0.50}$	$4.78^{+5.22}_{-3.49}$	$5.95^{+0.83}_{-1.37}$	$9.30^{+0.70}_{-5.48}$	$9.04^{+0.96}_{-3.95}$	$8.19^{+1.81}_{-4.68}$	$4.92^{+1.12}_{-2.36}$	$4.60^{+2.71}_{-2.04}$
v_A	[km/s]	$6.80^{+1.18}_{-2.73}$	$29.2^{+2.80}_{-1.47}$	$21.2^{+38.8}_{-21.2}$	$1.84^{+2.36}_{-1.08}$	$20.2^{+3.26}_{-6.33}$	$18.2^{+3.15}_{-5.91}$	$25.0^{+0.92}_{-2.30}$	$22.8^{+1.46}_{-1.05}$	$20.7^{+1.14}_{-3.43}$
$v_{0,c}$	[km/s]	$40.9^{+59.1}_{-5.89}$	$40.2^{+38.1}_{-25.2}$	$5.82^{+94.2}_{-5.82}$	$87.8^{+12.2}_{-7.57}$	$69.7^{+22.0}_{-24.7}$	$57.3^{+41.1}_{-12.3}$	$44.0^{+8.4}_{-16.5}$	-	-
z_h	[kpc]	$3.77^{+3.23}_{-1.77}$	$2.04^{+0.40}_{-0.04}$	$4.22^{+2.78}_{-2.22}$	$6.55^{+0.45}_{-1.63}$	$5.43^{+1.57}_{-3.43}$	$5.84^{+1.16}_{-3.84}$	$6.00^{+1.00}_{-4.00}$	$5.05^{+1.95}_{-3.05}$	$4.12^{+2.88}_{-2.12}$
ϕ_{AMS}		300^{+60}_{-80}	780^{+80}_{-40}	620^{+180}_{-195}	580^{+45}_{-115}	400^{+90}_{-40}	360^{+115}_{-45}	700^{+20}_{-50}	640^{+20}_{-20}	340^{+45}_{-125}

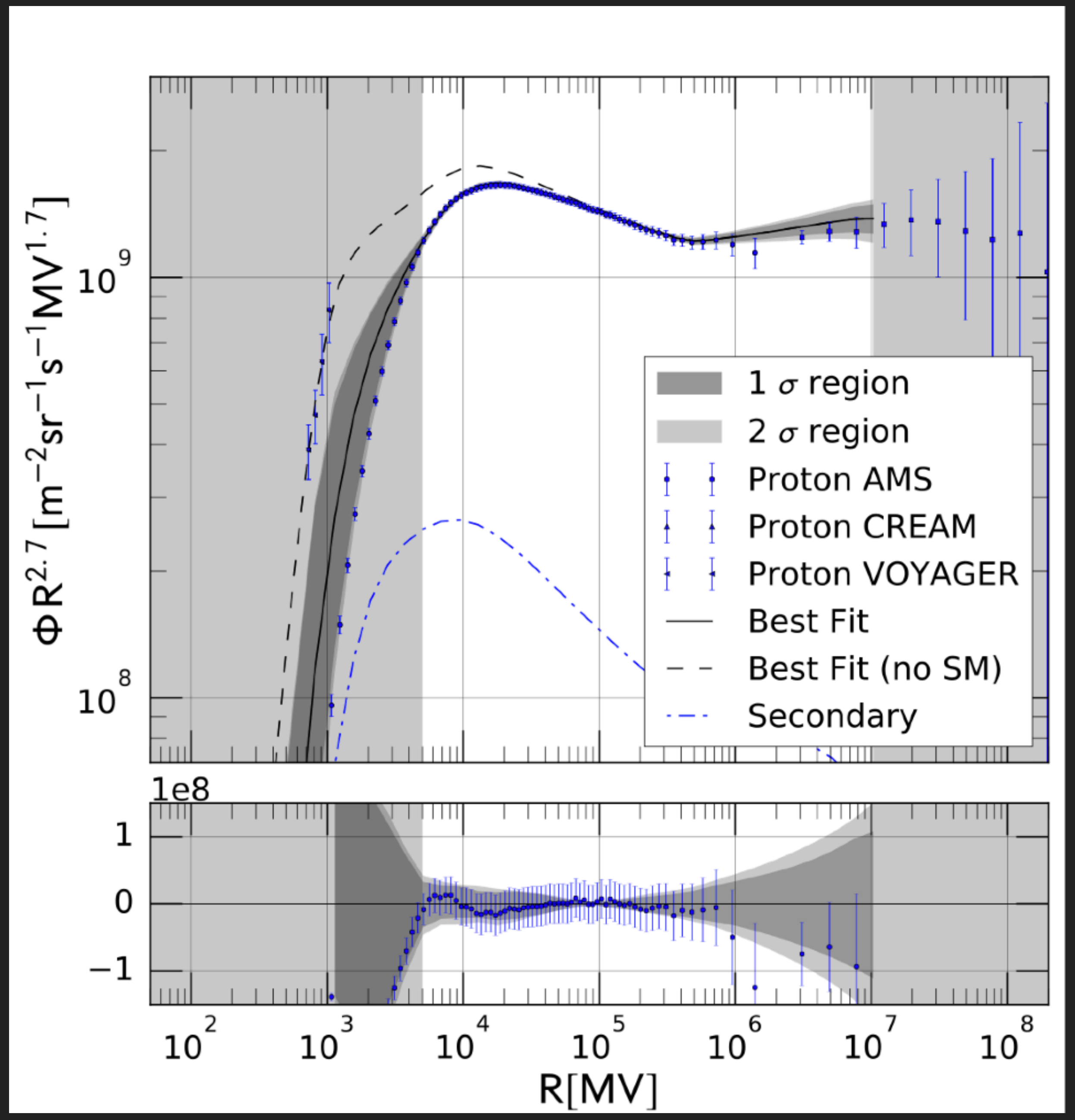

- Assume CR propagation is homogeneous.
- Fit data to local AMS-02 observables.

- It's about the sources.

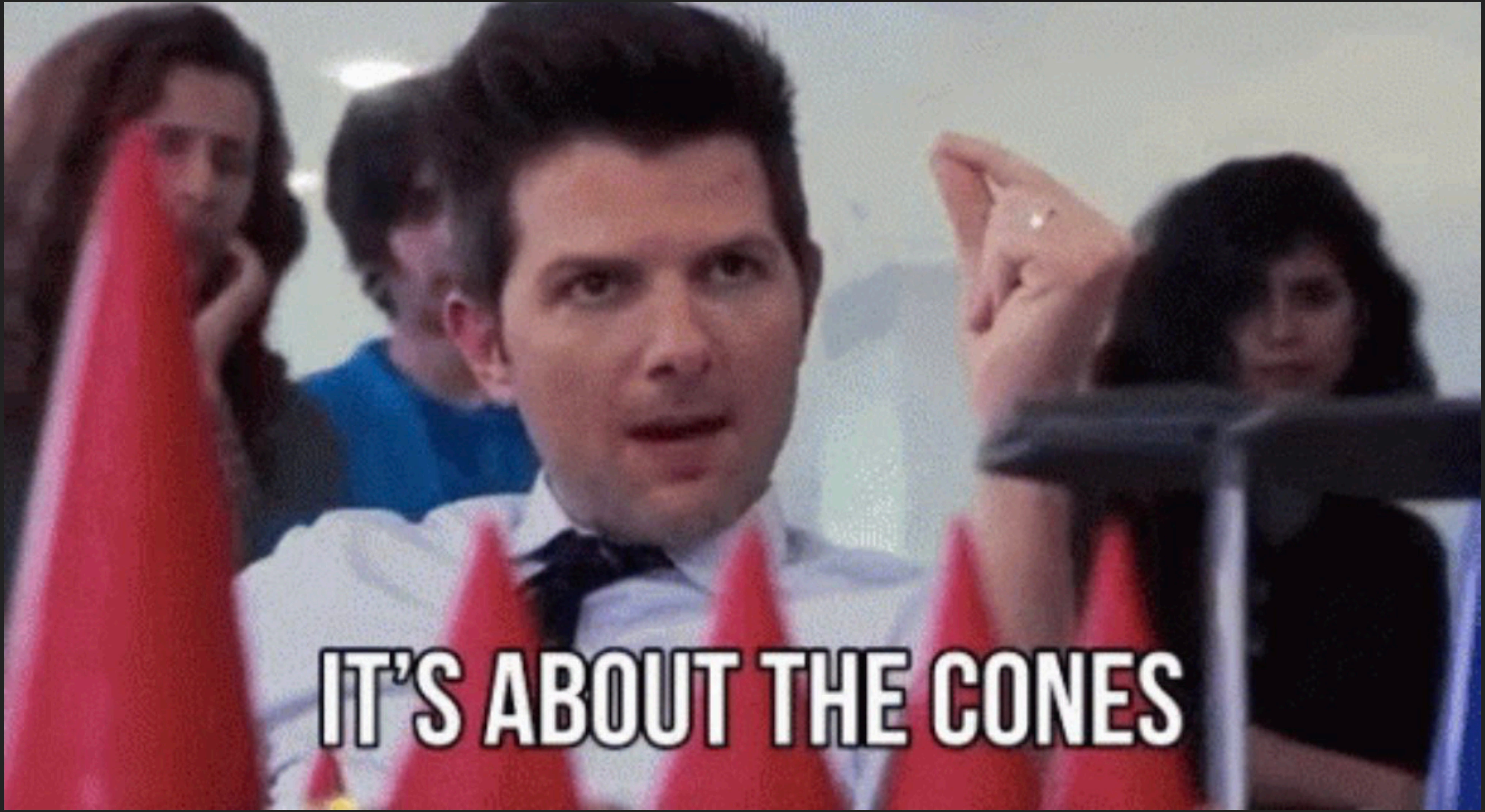

TEV HALOS SOLVE COSMIC-RAY DIFFUSION

- Pulsar catalogs provide an answer:
  - >3000 pulsars
  - Specific locations, ages, and spin down powers
  - Translates directly into local diffusion model in streaming instability models.

#	PSRJ	P0 (s)	P1	DIST (kpc)	AGE (Yr)	BSURF (G)	EDOT (ergs/s)
1	J0537-6910	0.016122	5.18e-14	49.700	4.93e+03	9.25e+11	4.88e+38
2	J0534+2200	0.033392	4.21e-13	2.000	1.26e+03	3.79e+12	4.46e+38
3	J0540-6919	0.050570	4.79e-13	49.700	1.67e+03	4.98e+12	1.46e+38
4	J1813-1749	0.044741	1.27e-13	4.700	5.58e+03	2.41e+12	5.60e+37
5	J1400-6325	0.031182	3.89e-14	7.000	1.27e+04	1.11e+12	5.07e+37
6	J1747-2809	0.052153	1.56e-13	8.141	5.31e+03	2.88e+12	4.33e+37
7	J1833-1034	0.061884	2.02e-13	4.100	4.85e+03	3.58e+12	3.37e+37
8	J2022+3842	0.048579	8.61e-14	10.000	8.94e+03	2.07e+12	2.96e+37
9	J0205+6449	0.065716	1.94e-13	3.200	5.37e+03	3.61e+12	2.70e+37
10	J2229+6114	0.051624	7.83e-14	3.000	1.05e+04	2.03e+12	2.25e+37
11	J1513-5908	0.151582	1.53e-12	4.400	1.57e+03	1.54e+13	1.73e+37
12	J1617-5055	0.069357	1.35e-13	4.743	8.13e+03	3.10e+12	1.60e+37
13	J1124-5916	0.135477	7.53e-13	5.000	2.85e+03	1.02e+13	1.19e+37
14	J1930+1852	0.136855	7.51e-13	7.000	2.89e+03	1.03e+13	1.16e+37
15	J1023-5746	0.111472	3.84e-13	2.080	4.60e+03	6.62e+12	1.09e+37
16	J1420-6048	0.068180	8.32e-14	5.632	1.30e+04	2.41e+12	1.04e+37
17	J1410-6132	0.050052	3.20e-14	13.510	2.48e+04	1.28e+12	1.01e+37
18	J1849-0001	0.038523	1.42e-14	*	4.31e+04	7.47e+11	9.78e+36
19	J1402+13	0.005890	4.83e-17	*	1.93e+06	1.71e+10	9.34e+36
20	J1846-0258	0.326571	7.11e-12	5.800	7.28e+02	4.88e+13	8.06e+36
21	J0835-4510	0.089328	1.25e-13	0.280	1.13e+04	3.38e+12	6.92e+36
22	J1811-1925	0.064667	4.40e-14	5.000	2.33e+04	1.71e+12	6.42e+36
23	J1111-6039	0.106670	1.95e-13	*	8.66e+03	4.62e+12	6.35e+36
24	J1813-1246	0.048072	1.76e-14	2.635	4.34e+04	9.30e+11	6.24e+36
25	J1838-0537	0.145708	4.72e-13	*	4.89e+03	8.39e+12	6.02e+36
26	J1838-0655	0.070498	4.92e-14	6.600	2.27e+04	1.89e+12	5.55e+36
27	J1418-6058	0.110573	1.69e-13	1.885	1.03e+04	4.38e+12	4.95e+36
28	J1935+2025	0.080118	6.08e-14	4.598	2.09e+04	2.23e+12	4.66e+36
29	J1856+0245	0.080907	6.21e-14	6.318	2.06e+04	2.27e+12	4.63e+36
30	J1112-6103	0.064962	3.15e-14	4.500	3.27e+04	1.45e+12	4.53e+36
31	J1640-4631	0.206443	9.76e-13	12.750	3.35e+03	1.44e+13	4.38e+36
32	J1844-0346	0.112855	1.55e-13	*	1.16e+04	4.23e+12	4.25e+36
33	J1952+3252	0.039531	5.84e-15	3.000	1.07e+05	4.86e+11	3.74e+36
34	J1826-1256	0.110224	1.21e-13	1.550	1.44e+04	3.70e+12	3.58e+36
35	J1709-4429	0.102459	9.30e-14	2.600	1.75e+04	3.12e+12	3.41e+36
36	J2021+3651	0.103741	9.57e-14	1.800	1.72e+04	3.19e+12	3.38e+36
37	J1524-5625	0.078219	3.90e-14	3.378	3.18e+04	1.77e+12	3.21e+36
38	J1357-6429	0.166108	3.60e-13	3.100	7.31e+03	7.83e+12	3.10e+36
39	J1913+1011	0.035909	3.37e-15	4.613	1.69e+05	3.52e+11	2.87e+36
40	J1826-1334	0.101487	7.53e-14	3.606	2.14e+04	2.80e+12	2.84e+36

Pulsar searches and timing with the square kilometre array

R. Smits[1], M. Kramer[1], B. Stappers[1], D. R. Lorimer[2,3], J. Cordes[4], and A. Faulkner[1]

[1] Jodrell Bank Centre for Astrophysics, University of Manchester, UK
e-mail: Roy.Smits@manchester.ac.uk
[2] Department of Physics, 210 Hodges Hall, West Virginia University, Morgantown, WV 26506, USA
[3] National Radio Astronomy Observatory, Green Bank, USA
[4] Astronomy Department, Cornell University, Ithaca, NY, USA

Received 13 June 2008 / Accepted 31 October 2008

ABSTRACT

The square kilometre array (SKA) is a planned multi purpose radio telescope with a collecting area approaching 1 million square metres. One of the key science objectives of the SKA is to provide exquisite strong-field tests of gravitational physics by finding and timing pulsars in extreme binary systems such as a pulsar-black hole binary. To find out how three preliminary SKA configurations will affect a pulsar survey, we have simulated SKA pulsar surveys for each configuration. We estimate that the total number of pulsars the SKA will detect, is around 14 000 normal pulsars and 6000 millisecond pulsars, using only the 1-km core and 30-mn integration time. We describe a simple strategy for follow-up timing observations and find that, depending on the configuration, it would take 1–6 days to obtain a single timing point for 14 000 pulsars. Obtaining one timing point for the high-precision timing projects of the SKA, will take less than 14 h, 2 days, or 3 days, depending on the configuration. The presence of aperture arrays will be of great benefit here. We also study the computational requirements for beam forming and data analysis for a pulsar survey. Beam forming of the full field of view of the single pixel feed 15-m dishes using the 1-km core of the SKA requires about 2.2×10^{15} operations

CONCLUSIONS

- TeV halos are a common feature around middle-aged (and possibly young and recycled pulsars).
- Understanding the earliest stages of TeV halo formation (or composite sources, if you prefer), is critical for understanding TeV halo evolution.
- We need physical models!
- TeV halos provide critical information that will be necessary to make detailed TeV emission models.

TEV HALOS SOLVE COSMIC-RAY DIFFUSION

Gaggero et al. (2014; 1411.7623)

- First attempts at this approach.
- Decreasing diffusion in the spiral arms produces better fits to GeV gamma-ray data

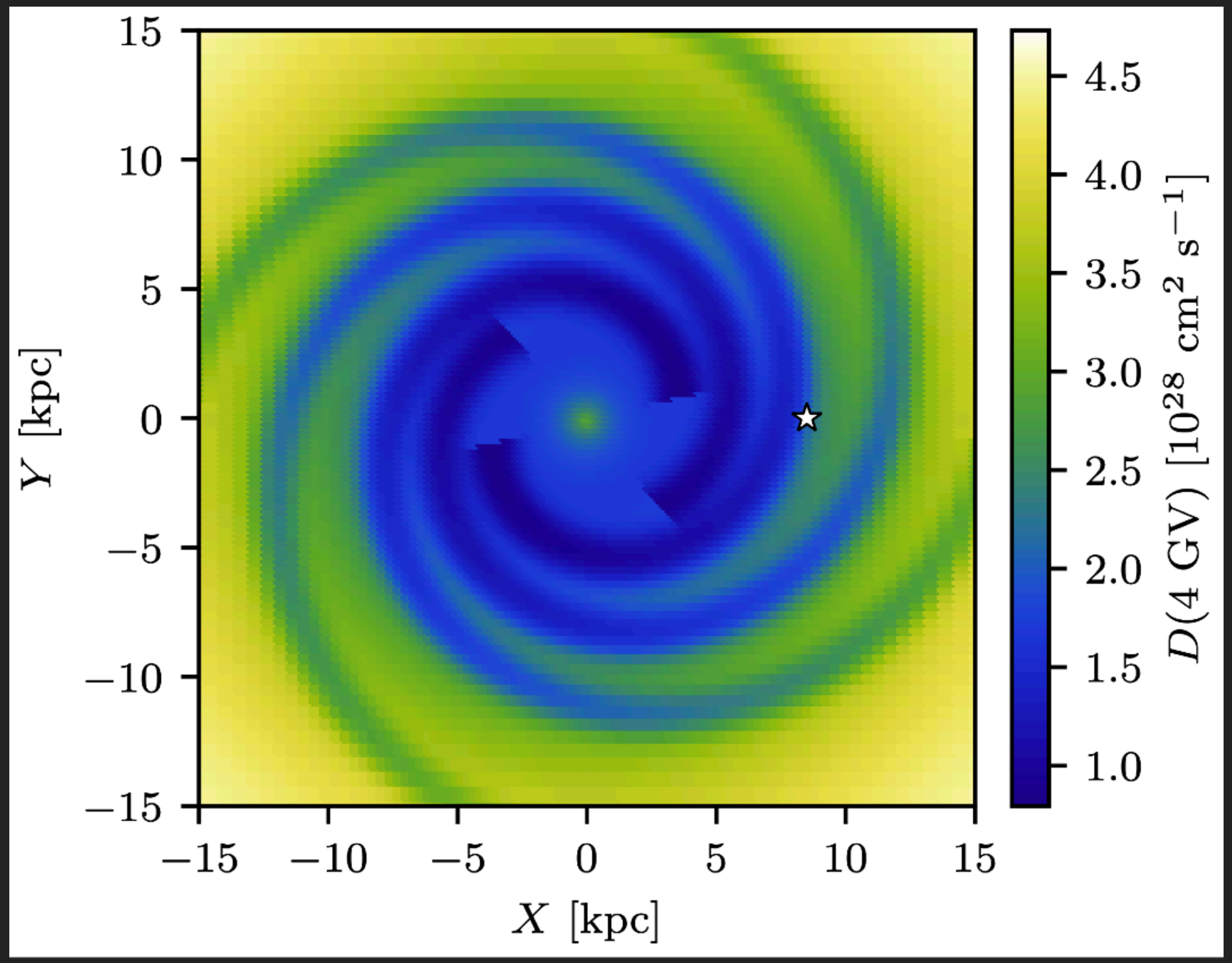

Jóhannesson et al. (2019.1903.05509)

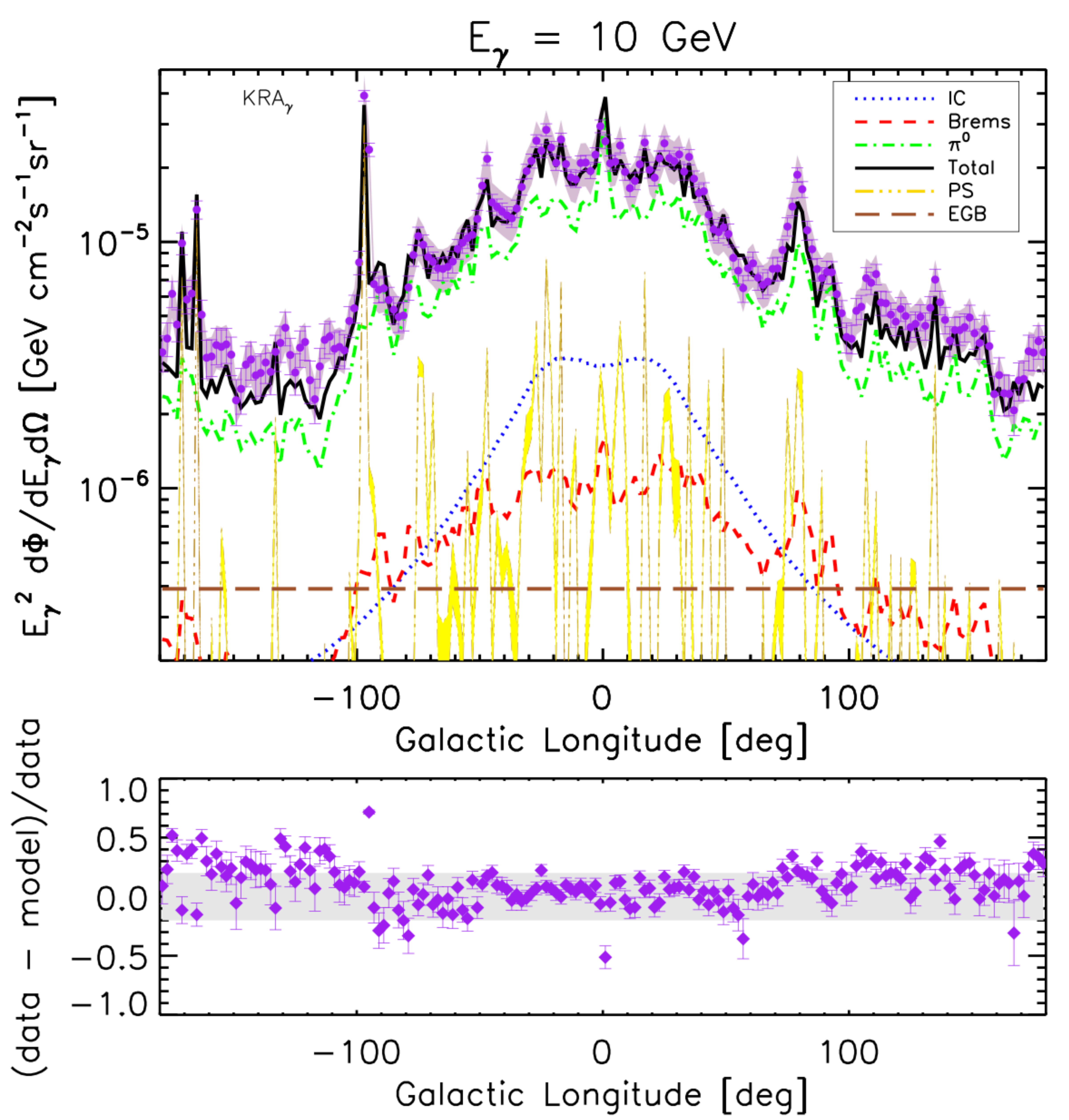

IMPLICATION: DIFFUSE TEV GAMMA-RAYS

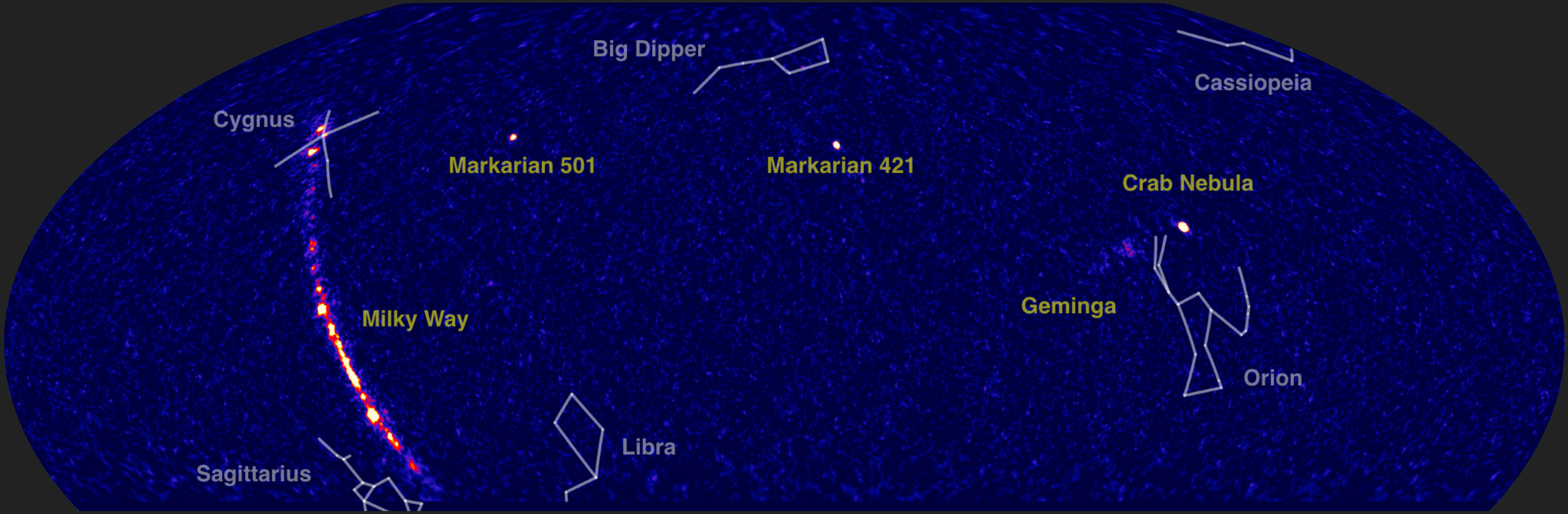

- There is bright diffuse gamma-ray emission across the galactic plane.

- Ratio of point source emission to diffuse emission is a powerful marker of emission mechanisms and local propagation.

IMPLICATION: MILAGRO DIFFUSE TEV EXCESS

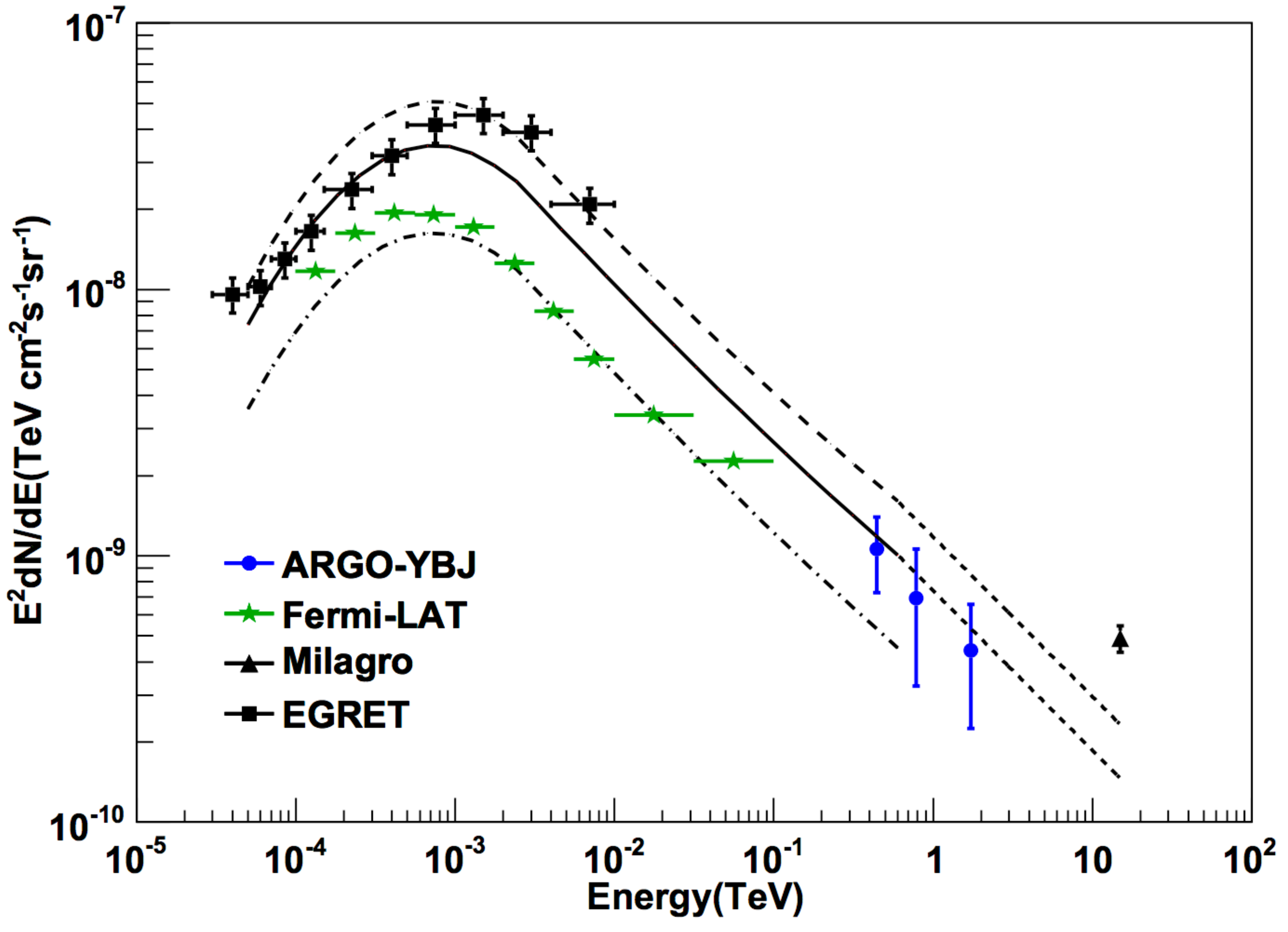

IMPLICATION: DIFFUSE TEV GAMMA-RAYS

Linden & Buckman (2017; 1707.01905)

- If all convert a similar fraction of their spin down power to e+e- pairs as Geminga, then TeV halos naturally explain this observation.

- Note - "Halo" is not needed
  - Pulsar efficiency ~10%
  - Power must escape PWN

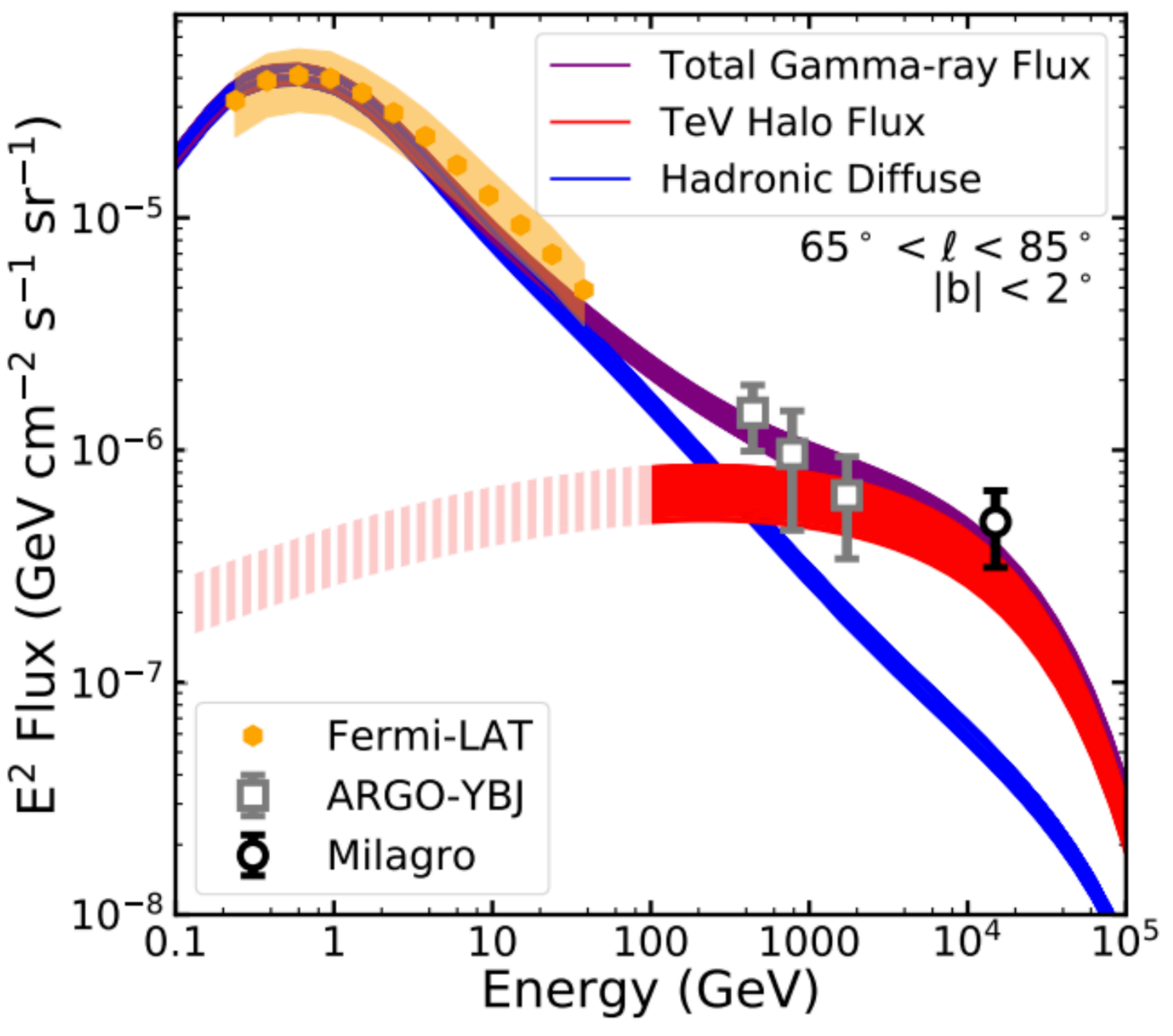

CONCLUSIONS - TEV GAMMA-RAY MODELING

- TeV halos are a common feature around middle-aged (and possibly young and recycled pulsars).

- Understanding the earliest stages of TeV halo formation (or composite sources, if you prefer), is critical for understanding TeV halo evolution.

- TeV halos provide critical information that will be necessary to make detailed TeV emission models.

- The Rise of the Leptons: PWN and TeV halo activity may dominate the diffuse TeV emission, important interplay between CTA/HAWC/LHAASO and IceCube.

DIFFERENCES IN DEFINITION

- If TeV halo power is connected to pulsar spin down power, we can build a model of the full TeV sky.

- This means that many young systems should also produce even brighter TeV halo activity!

#	PSRJ	P0 (s)	P1	DIST (kpc)	AGE (Yr)	BSURF (G)	EDOT (ergs/s)
1	J0537-6910	0.016122	5.18e-14	49.700	4.93e+03	9.25e+11	4.88e+38
2	J0534+2200	0.033392	4.21e-13	2.000	1.26e+03	3.79e+12	4.46e+38
3	J0540-6919	0.050570	4.79e-13	49.700	1.67e+03	4.98e+12	1.46e+38
4	J1813-1749	0.044741	1.27e-13	4.700	5.58e+03	2.41e+12	5.60e+37
5	J1400-6325	0.031182	3.89e-14	7.000	1.27e+04	1.11e+12	5.07e+37
6	J1747-2809	0.052153	1.56e-13	8.141	5.31e+03	2.88e+12	4.33e+37
7	J1833-1034	0.061884	2.02e-13	4.100	4.85e+03	3.58e+12	3.37e+37
8	J2022+3842	0.048579	8.61e-14	10.000	8.94e+03	2.07e+12	2.96e+37
9	J0205+6449	0.065716	1.94e-13	3.200	5.37e+03	3.61e+12	2.70e+37
10	J2229+6114	0.051624	7.83e-14	3.000	1.05e+04	2.03e+12	2.25e+37
11	J1513-5908	0.151582	1.53e-12	4.400	1.57e+03	1.54e+13	1.73e+37
12	J1617-5055	0.069357	1.35e-13	4.743	8.13e+03	3.10e+12	1.60e+37
13	J1124-5916	0.135477	7.53e-13	5.000	2.85e+03	1.02e+13	1.19e+37
14	J1930+1852	0.136855	7.51e-13	7.000	2.89e+03	1.03e+13	1.16e+37
15	J1023-5746	0.111472	3.84e-13	2.080	4.60e+03	6.62e+12	1.09e+37
16	J1420-6048	0.068180	8.32e-14	5.632	1.30e+04	2.41e+12	1.04e+37
17	J1410-6132	0.050052	3.20e-14	13.510	2.48e+04	1.28e+12	1.01e+37
18	J1849-0001	0.038523	1.42e-14	*	4.31e+04	7.47e+11	9.78e+36
19	J1402+13	0.005890	4.83e-17	*	1.93e+06	1.71e+10	9.34e+36
20	J1846-0258	0.326571	7.11e-12	5.800	7.28e+02	4.88e+13	8.06e+36
21	J0835-4510	0.089328	1.25e-13	0.280	1.13e+04	3.38e+12	6.92e+36
22	J1811-1925	0.064667	4.40e-14	5.000	2.33e+04	1.71e+12	6.42e+36
23	J1111-6039	0.106670	1.95e-13	*	8.66e+03	4.62e+12	6.35e+36
24	J1813-1246	0.048072	1.76e-14	2.635	4.34e+04	9.30e+11	6.24e+36
25	J1838-0537	0.145708	4.72e-13	*	4.89e+03	8.39e+12	6.02e+36
26	J1838-0655	0.070498	4.92e-14	6.600	2.27e+04	1.89e+12	5.55e+36
27	J1418-6058	0.110573	1.69e-13	1.885	1.03e+04	4.38e+12	4.95e+36
28	J1935+2025	0.080118	6.08e-14	4.598	2.09e+04	2.23e+12	4.66e+36
29	J1856+0245	0.080907	6.21e-14	6.318	2.06e+04	2.27e+12	4.63e+36
30	J1112-6103	0.064962	3.15e-14	4.500	3.27e+04	1.45e+12	4.53e+36
31	J1640-4631	0.206443	9.76e-13	12.750	3.35e+03	1.44e+13	4.38e+36
32	J1844-0346	0.112855	1.55e-13	*	1.16e+04	4.23e+12	4.25e+36
33	J1952+3252	0.039531	5.84e-15	3.000	1.07e+05	4.86e+11	3.74e+36
34	J1826-1256	0.110224	1.21e-13	1.550	1.44e+04	3.70e+12	3.58e+36
35	J1709-4429	0.102459	9.30e-14	2.600	1.75e+04	3.12e+12	3.41e+36
36	J2021+3651	0.103741	9.57e-14	1.800	1.72e+04	3.19e+12	3.38e+36
37	J1524-5625	0.078219	3.90e-14	3.378	3.18e+04	1.77e+12	3.21e+36
38	J1357-6429	0.166108	3.60e-13	3.100	7.31e+03	7.83e+12	3.10e+36
39	J1913+1011	0.035909	3.37e-15	4.613	1.69e+05	3.52e+11	2.87e+36
40	J1826-1334	0.101487	7.53e-14	3.606	2.14e+04	2.80e+12	2.84e+36

MANY CAVEATS

IceCube Collaboration (2023)

- IceCube neutrino flux is unknown at low energies (nearly order of magnitude uncertainties from models that fit the data to within 1σ.
- On top of this, there is an intrinsic factor of 2 uncertainty in even the IceCube flux measurement.
- There is also a factor of ~2 uncertainty in the TeV halo flux owing to the "Geminga-like" assumption

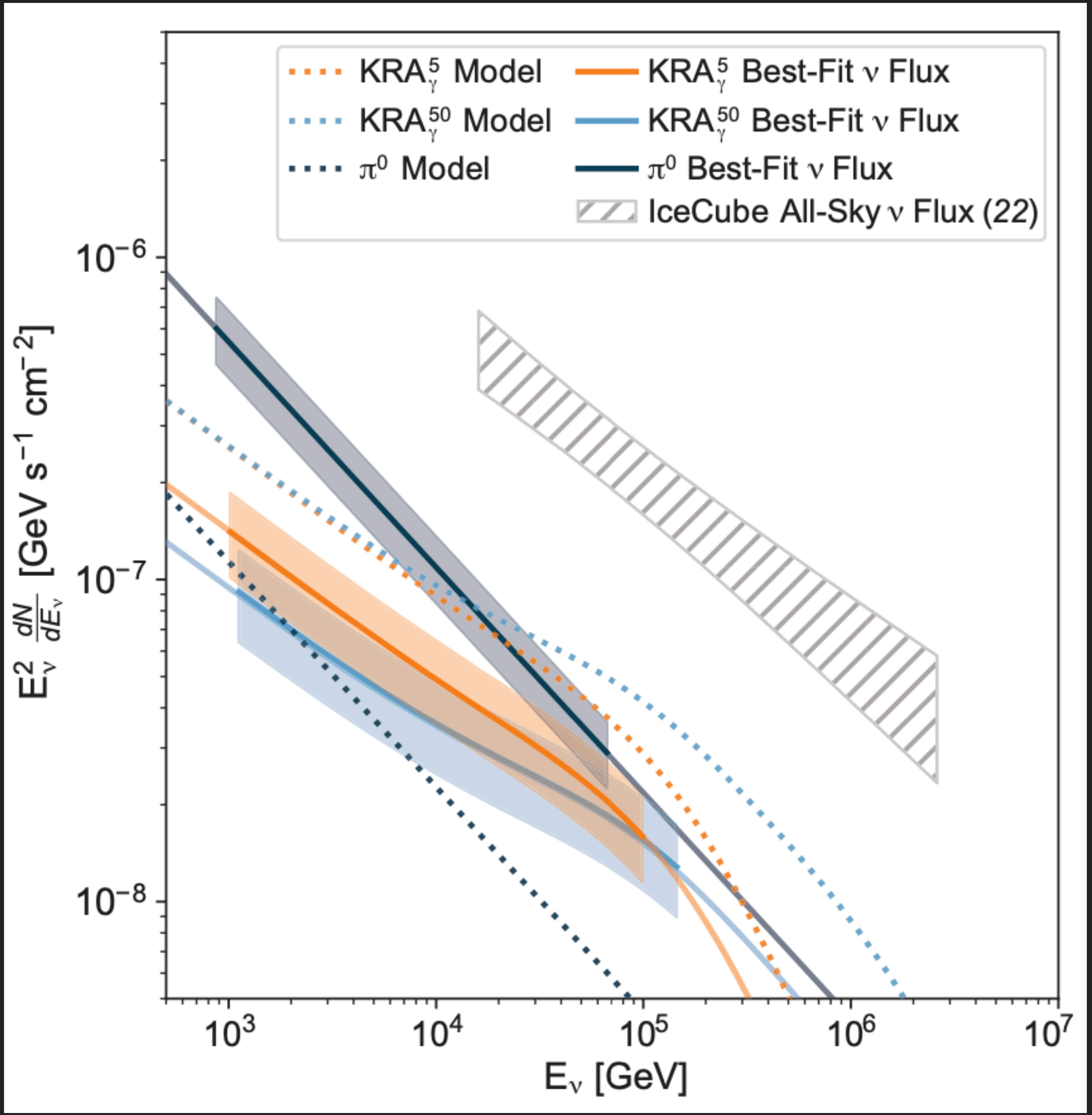

ASSUMPTION: AN EQUIVALENT E+E- POWER FOR ALL PULSARS

- Observations of Geminga and Monogem indicate that they convert ~10% of their spindown power to e+e- pairs that escape the PWN.
- We assume this is generic for all pulsars, but examine significant changes in pulsar parameters.

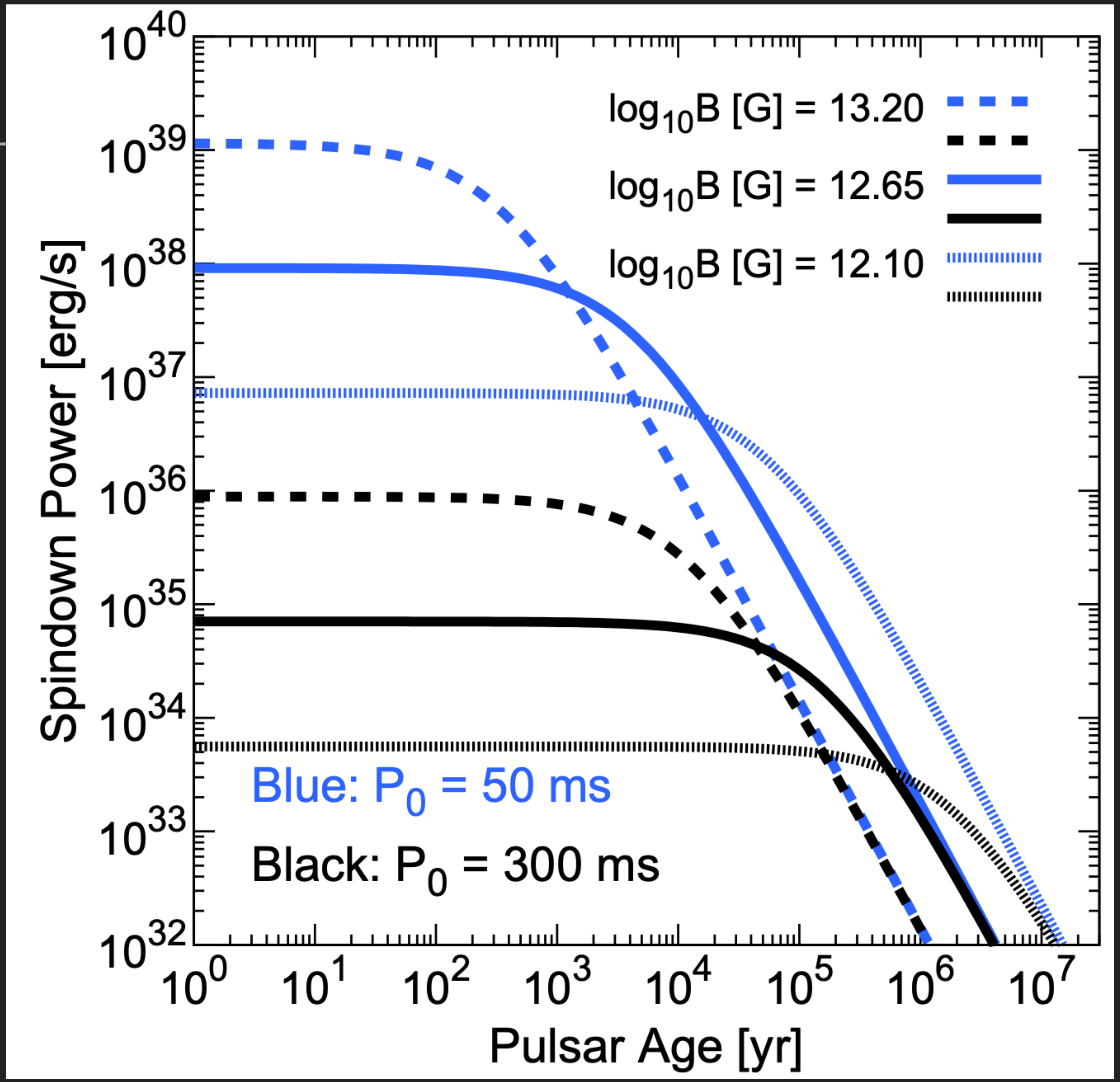

Sudoh, TL, Beacom (2019; 1902.08203)

Linden et al. (2017; 1703.09704)

ATNF Name	Dec. (°)	Distance (kpc)	Age (kyr)	Spindown Lum. (erg s^{-1})	Spindown Flux (erg s^{-1} kpc^{-2})	2HWC
J0633+1746	17.77	0.25	342	3.2e34	4.1e34	2HWC J0631+169
B0656+14	14.23	0.29	111	3.8e34	3.6e34	2HWC J0700+143
B1951+32	32.87	3.00	107	3.7e36	3.3e34	—
J1740+1000	10.00	1.23	114	2.3e35	1.2e34	—
J1913+1011	10.18	4.61	169	2.9e36	1.1e34	2HWC J1912+099
J1831-0952	-9.86	3.68	128	1.1e36	6.4e33	2HWC J1831-098
J2032+4127	41.45	1.70	181	1.7e35	4.7e33	2HWC J2031+415
B1822-09	-9.58	0.30	232	4.6e33	4.1e33	—
B1830-08	-8.45	4.50	147	5.8e35	2.3e33	—
J1913+0904	9.07	3.00	147	1.6e35	1.4e33	—
B0540+23	23.48	1.56	253	4.1e34	1.4e33	—

OPEN QUESTION: MSP HALOS?

Hooper, TL (2021; 2104.00014)

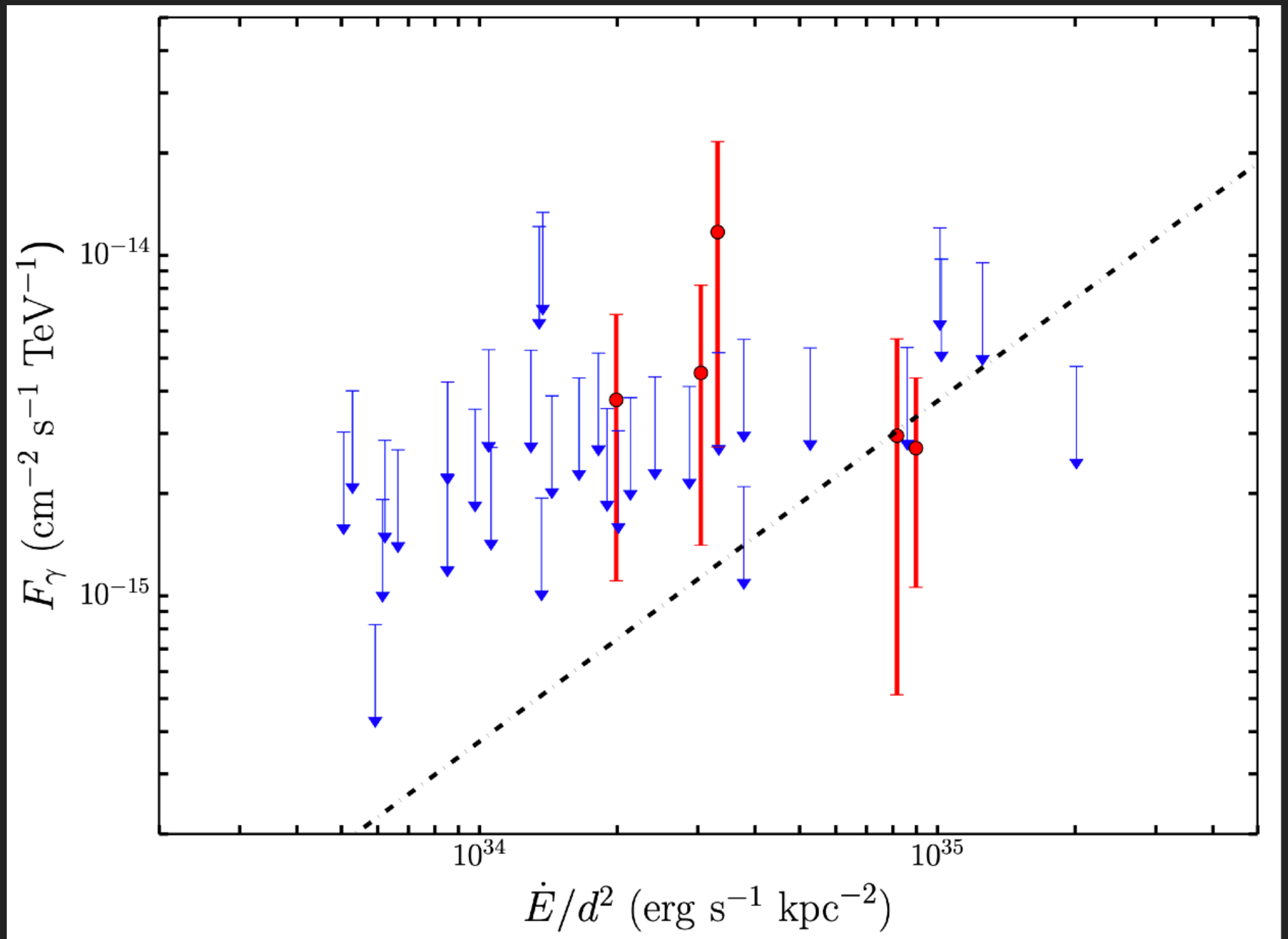

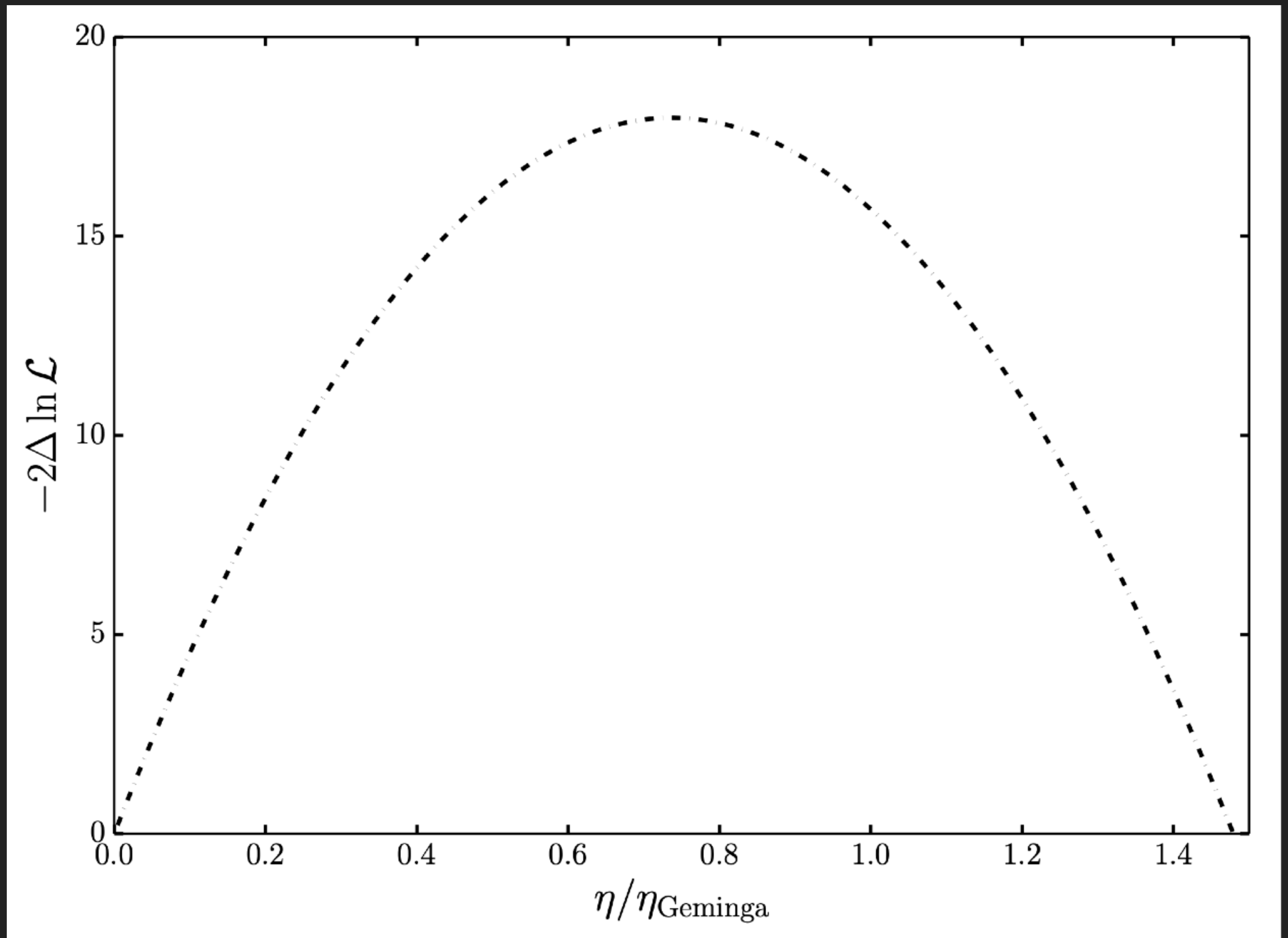

- Do MSPs Have TeV Halos?
- Tentative: 4.24σ Poisson evidence from a HAWC stacking analysis (~2.3σ from blank sky test).
- Possible MSP Detection by LHAASO
- Important theoretical implications:
  - Cosmic-Ray confinement near pulsars?
  - Cosmic-Ray diffusion at high latitudes
  - PWN/Magnetospheric acceleration models.

LHAASO Collaboration (2023; 2305.17030)

1LHAASO J0216+4237u	0.33	ATNF PSR J0218+4232	$\dot{E} = 2.44 \times 10^{35}$ erg s^{-1},τ_c = 476000.0 kyr,d = 3.15 kpc
	0.33	4FGL J0218.1+4232	PSR J0218+4232;MSP;

- But propagation is not homogeneous.
- Local TeV observations might not tell you anything!

TEV HALOS SOLVE COSMIC-RAY DIFFUSION

Porter et al. (2019; 1909.02223)
See also: Thaler et al. (2022 2209.02295)

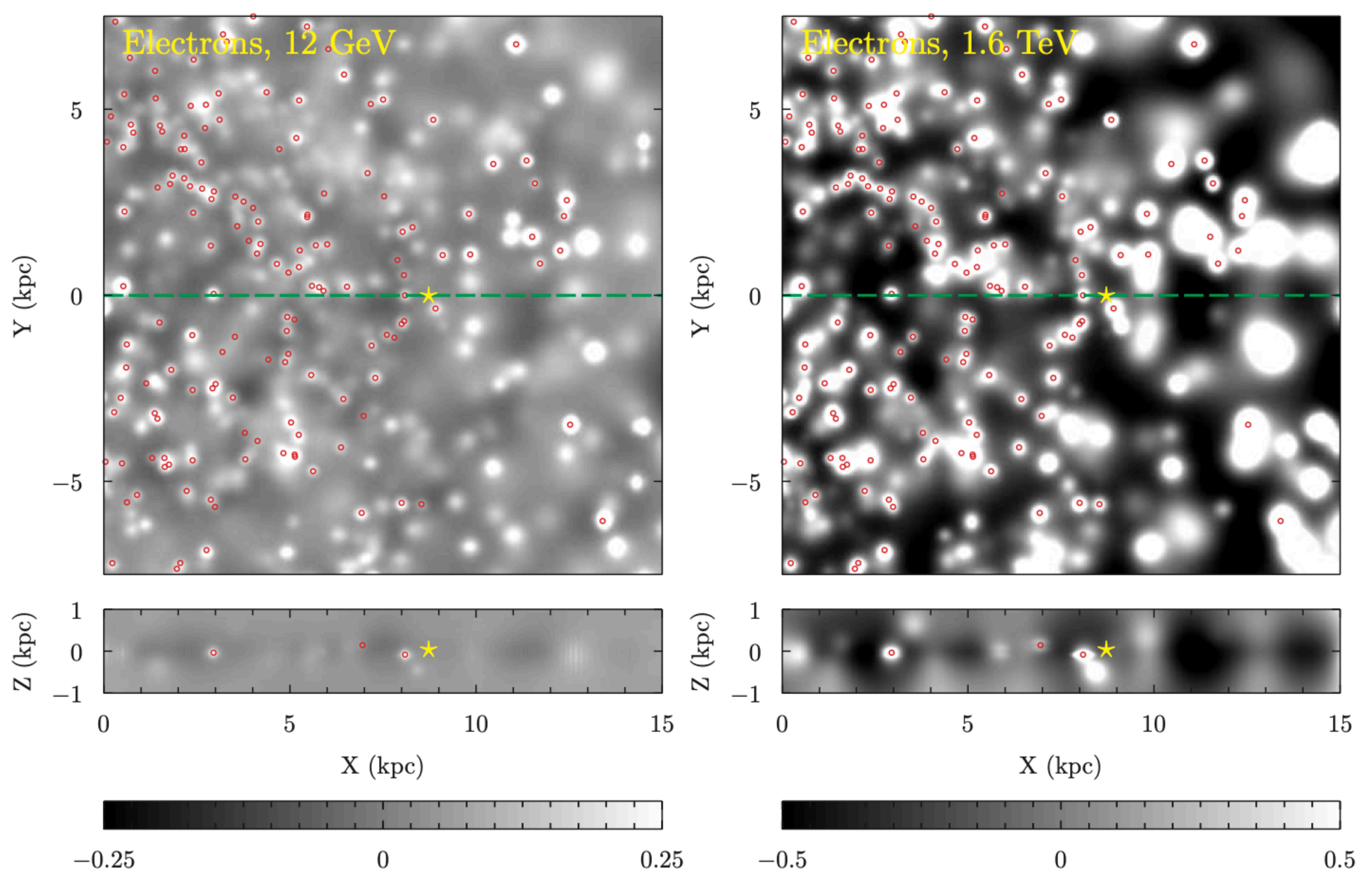

The GALPROP Cosmic-ray Propagation and Nonthermal Emissions Framework: Release v57

T. A. Porter[1], G. Jóhannesson[2], and I. V. Moskalenko[1]
[1] W.W. Hansen Experimental Physics Laboratory and Kavli Institute for Particle Astrophysics and Cosmology, Stanford University, Stanford, CA 94305, USA
tporter@stanford.edu
[2] Science Institute, University of Iceland, IS-107 Reykjavik, Iceland
Received 2021 December 22; revised 2022 July 10; accepted 2022 July 12; published 2022 September 9

Abstract

The past decade has brought impressive advances in the astrophysics of cosmic rays (CRs) and multiwavelength astronomy, thanks to the new instrumentation launched into space and built on the ground. Modern technologies employed by those instruments provide measurements with unmatched precision, enabling searches for subtle signatures of dark matter and new physics. Understanding the astrophysical backgrounds to better precision than the observed data is vital in moving to this new territory. A state-of-the-art CR propagation code, called GALPROP, is designed to address exactly this challenge. Having 25 yr of development behind it, the GALPROP framework has become a de facto standard in the astrophysics of CRs, diffuse photon emissions (radio to γ-rays), and searches for new physics. GALPROP uses information from astronomy, particle physics, and nuclear physics to predict CRs and their associated emissions self-consistently, providing a unifying modeling framework. The range of its physical validity covers 18 orders of magnitude in energy, from sub-keV to PeV energies for particles and from μeV to PeV energies for photons. The framework and the data sets are public and are extensively used by many experimental collaborations and by thousands of individual researchers worldwide for interpretation of their data and for making predictions. This paper details the latest release of the GALPROP framework and updated cross sections, further developments of its initially auxiliary data sets for models of the interstellar medium that grew into independent studies of the Galactic structure—distributions of gas, dust, radiation, and magnetic fields—as well as the extension of its modeling capabilities. Example applications included with the distribution illustrating usage of the new

IMPLICATION: DIFFUSE TEV GAMMA-RAYS

- TeV halos naturally explain the spectrum and intensity of this emission.
- Multiple halos observed with $E^{-2.0}$ spectra.

- Note - “Halo” is not needed
  - Pulsar efficiency ~10%
  - Power must escape PWN

Yan & Liu (2023; 2304.12574)

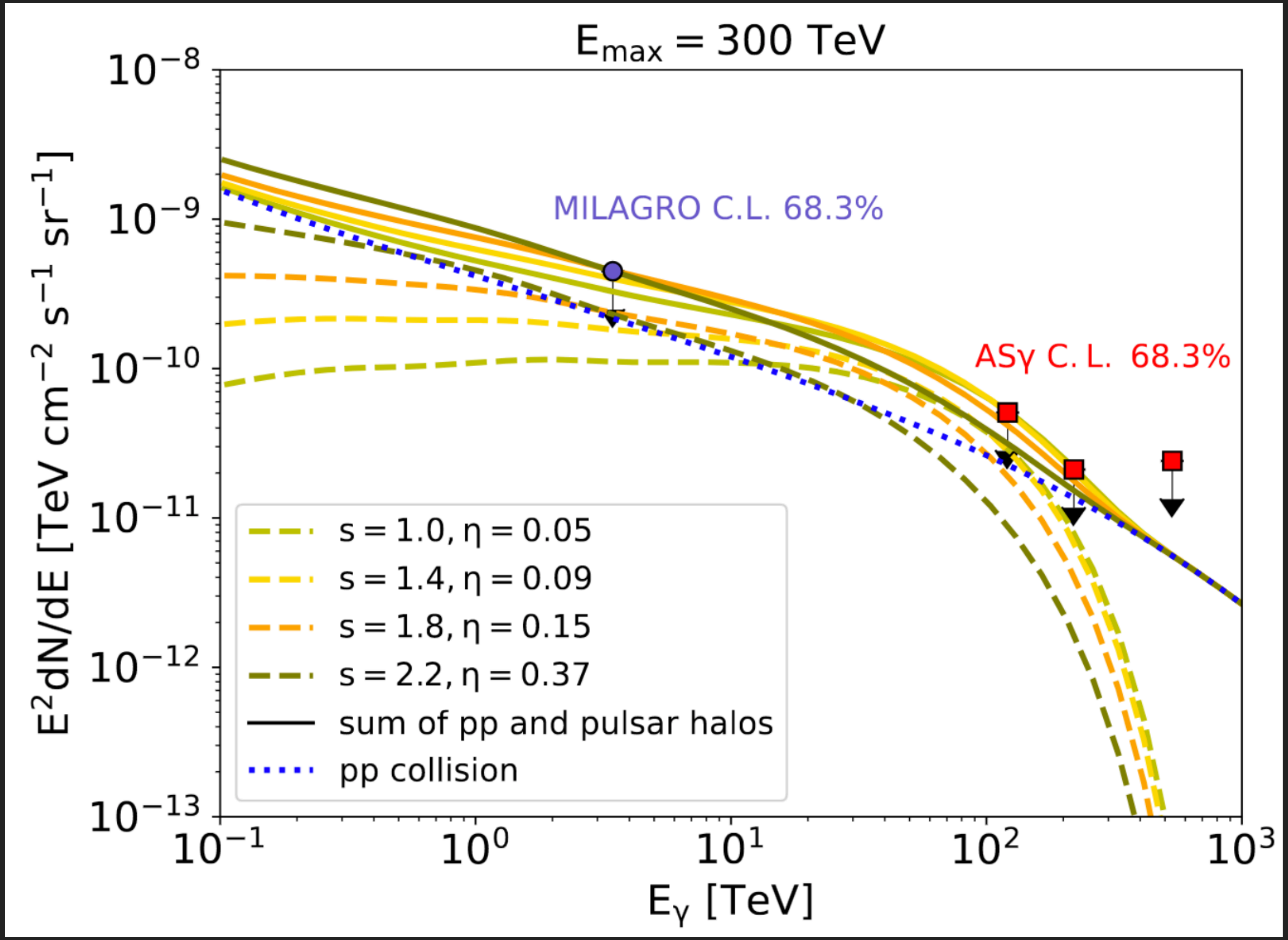

LHAASO Data

TEV HALOS BREAK GEV GAMMA-RAY DIFFUSE EMISSION MODELS

Widmark et al. (2022; 2208.11704)

- Target models come from gas and dust tracers.
- CR density comes from Galprop simulations.